Supporting Information

Simple Bifunctional Salts for Synthesising Block Copolymers from Anhydrides/Epoxides and Vinyl Acetate

Anna Lykkeberg[a] and Jennifer A. Garden*[a]

[a]EaStCHEM School of Chemistry, The University of Edinburgh, UK

Email address: j.garden@ed.ac.uk

Table of Contents

Experimental

General Experimental Details

All manipulations involving air- or moisture-sensitive compounds were performed either in a glove box or using standard Schlenk techniques under an argon atmosphere. All reagents and solvents were purchased from Sigma-Aldrich, Fisher Scientific and Fluorochem, and used without further purification unless stated otherwise. Dry toluene was collected from a solvent purification system (Innovative Technologies), dried over activated 4 Å molecular sieves and stored under argon. $CDCl_3$ was degassed three times by freeze-pump-thaw and then stored over activated 4 Å molecular sieves under argon. Phthalic anhydride was purified by recrystallisation and hot filtration from chloroform, followed by sublimation before storing in a glovebox under argon. Cyclohexene oxide was stirred over CaH_2 overnight before vacuum distilling and storing in a glovebox under argon. Epoxybutane was stirred over CaH_2 overnight, degassed three times by freeze-pump-thaw and then vacuum transferred before storing in a glovebox under argon.

^1H, ^{13}C and 2D NMR (COSY, HSQC, HMBC) were recorded on Bruker AVA400, AVA500 or AVA600 spectrometers at 300 K operating at 400 MHz, 500 MHz and 600 MHz respectively. Chemical shifts (δ) are given in ppm, and coupling constants (*J*) are reported in Hertz (Hz). Integration is provided and assignments are indicated. ^1H and ^{13}C NMR spectra were referenced with respect to the residual peaks of deuterated solvents, for ^{13}C spectra using D_2O, 2 µL of MeOH was added as a reference[1] ($CDCl_3$: 7.27 ppm, 77.0 ppm; D_2O: 4.79 ppm, MeOH 49.50 ppm). Multiplicities are indicated by s (singlet), d (doublet), t (triplet), q (quartet). DOSY NMR experiments were performed at 300 K on a Bruker Ascend 2 channel instrument operating at a frequency of 500 MHz and equipped with a z-gradient DCH/5 mm tuneable "CryoProbe"™ probe and a GRASP II gradient spectroscopy accessory providing a maximum gradient output of 53.5 G/cm. The dstebpg3s pulse program was used with a delay time (Δ) of 0.1 s and a gradient length (δ) of 1500 µs. A relaxation delay of 2 s was employed along with a longitudinal eddy current delay (LED) of 5 ms. Bipolar gradients pulses ($\delta/2$) of 1.5 ms and homospoil gradient pulses of 0.6 ms were used. The gradient strengths of the 3 homospoil pulses were -13.17%, -17.13%, -15.37%. 16 experiments were collected with the bipolar gradient strength, initially at 5% (1st experiment), linearly increased to 95% (16th experiment). All gradient pulses were smooth-square shaped (SMSQ10.100) and after each application a recovery delay of 200 µs used. The experiment was run with 16 scans per increment, employing one stimulated echo with two spoiling gradients. DOSY plots were generated using Bruker software TopSpin (4.40) and Dynamic Centre (2.8.4).

For SEC, polymer samples (2 – 10 mg) were dissolved in SEC grade THF (1 mL) and filtered using a 0.2 µm PTFE syringe filter. SEC analyses of the filtered polymer samples were carried out in SEC grade THF at a flow rate of 1 mL min^{-1} at 35 °C on an Agilent 1260 Infinity II GPC/SEC single detector system with mixed bed C PLgel columns (300 x 7.5 mm). The RI detector was calibrated using a narrow molecular weight polystyrene standards. SEC fractionation was carried out by collecting 1 minute fractions as the sample eluted, and repeating this process several times until enough material was obtained for NMR characterisation.

Attenuated total reflectance fourier transform infrared spectroscopy (ATR-FTIR) was measured on a Shimadzu IRSpirit with a QATR-S Single Reflectron ATR accessory.

MALDI-ToF MS analyses were performed using a Bruker Daltonics UltrafleXtreme™ instrument with a double time-of-flight (ToF) mass analyser (MALDI-ToF/ToF MS) in either reflectron positive (RP) or linear positive (LP) mode. Calibration was performed in either RP or LP mode against a 10 mg mL^{-1} solution of red phosphorus in THF. Data are reported in the form of m/z. The sample to be analysed,

dithranol matrix and sodium trifluoroacetic acid were dissolved in THF at 10 mg mL^{-1} and the solutions were mixed in a 2:2:1 ratio. A droplet (2 µL) of the resultant mixture was spotted on to the sample plate and submitted for MALDI-ToF MS analysis.

Synthesis of L_1H

Ligand **L_1H** was synthesised using an adapted literature procedure.[2] Potassium ethyl xanthogenate (21.16 g, 132 mmol) was stirred in acetone (160 mL) at 0 °C for 15 minutes, prior to the dropwise addition of bromoacetic acid (15.56 g, 112 mmol) dissolved in acetone (40 mL) over 20 minutes. The reaction was warmed to room temperature and left stirring overnight (18 hours) affording a pale peach suspension. The mixture was filtered and the filtrate concentrated *in vacuo*. The dark yellow liquid was dissolved in dichloromethane (100 mL) and washed twice with brine (2 x 50 mL). The dichloromethane fraction was dried over $MgSO_4$ and concentrated *in vacuo*. The dark yellow liquid was triturated with cold hexane (30 mL) to give a pale brown solid. The crude product was recrystallised from hexane to produce colourless needles (5.88 g, 29%).

^{1}H NMR (500 MHz, $CDCl_3$, 300 K): δ 4.67 (q, 2H, *J* = 7.1 Hz), 3.98 (s, 2H), 1.43 (t, 3H, *J* = 7.1 Hz)

^{1}H NMR (500 MHz, D_2O, 300 K): δ 4.72 (q, 2H, *J* = 7.1 Hz), 4.01 (s, 2H), 1.43 (t, 3H, 7.1 Hz)

^{13}C NMR (126 MHz, D_2O, 300 K): δ 214.8, 172.8, 75.0, 43.5, 12.8

Synthesis of L_2H

The synthesis of **L_2H** was adapted from a literature procedure.[3] Bromopropionic acid (5.6 mL, 62 mmol) was stirred in acetone (80 mL) at 0 °C for 15 minutes. Potassium ethyl xanthogenate (10.58 g, 66 mmol) was subsequently added over 20 minutes. The reaction was then warmed to room temperature and was stirred overnight (18 hours). The reaction was filtered and the filtrate concentrated *in vacuo*. The brown liquid was dissolved in dichloromethane (30 mL) and washed with deionised water (40 mL) and brine (40 mL). The organic layer was concentrated *in vacuo*, and the crude product was precipitated from cold pentane. The product was recrystallised from hexane to give an off-white solid (1.22 g, 10%).

^{1}H NMR (500 MHz, $CDCl_3$, 300 K): δ 4.65 (qd, 2H, J_q = 7.1 Hz, J_d = 1.8 Hz), 4.42 (q, 1H, *J* = 7.4 Hz), 1.61 (d, 3H, *J* = 7.4 Hz), 1.42 (t, 3H, *J* = 7.1 H)

^{13}C NMR (126 MHz, $CDCl_3$, 300 K): δ 213.5, 176.9, 70.7, 46.9, 16.7, 13.4

Synthesis routes to prepare LM

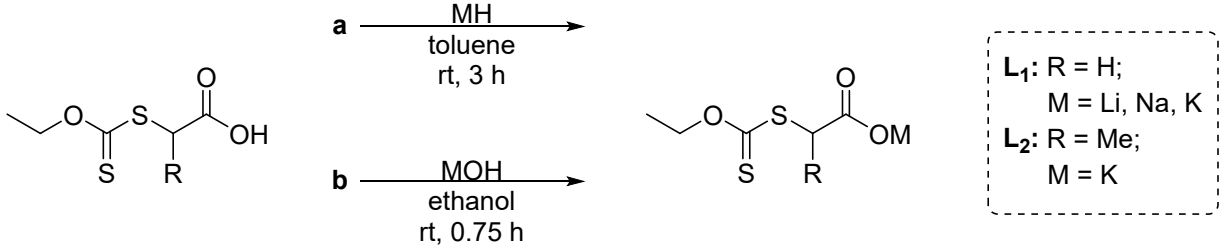

Upon deprotonation of **L_1H**, the ^{1}H NMR spectra showed a clear shift for the C*H*$_2$-CO_2 protons, from 4.01 ppm to 3.80 ppm for **L_1K,** δ = 3.83 ppm for **L_1Na** and δ = 3.81 ppm for **L_1Li** (D_2O solvent, refer to ESI). With **L_2H** and **L_2K** a solubility change was observed; **L_2H** was analysed in $CDCl_3$, whereas the salt **L_2K** required more polar D_2O. Elemental analysis further confirmed the formation of **L_1M** and **L_2K**.

Successful synthesis of the **L_1M** salts *via* the MOH route (route b) was evidenced by the identical ^{1}H NMR spectra obtained *via* the MH and MOH routes. IR analysis showed the loss of the OH stretches and a shift from the **L_1H** carbonyl stretch (1698 cm^{-1}) to **L_1M** carboxylate stretches (1384 cm^{-1} and 1575 cm^{-1} for **L_1K**).

Route a: Glovebox Synthesis of LM

As a representative synthesis for **L_1K**, in a glovebox, **L_1H** (180.3 mg, 1 mmol) was dissolved in toluene (15 mL) and KH (40.1 mg, 1 mmol) was added slowly over 10-15 minutes. After three hours at room temperature under argon atmosphere, the reaction was concentrated *in vacuo* giving a white powder (162.5 mg, 74%).

^{1}H NMR (500 MHz, D_2O, 300 K): δ 4.71 (q, 2H, *J* = 7.2 Hz), 3.80 (s, 2H), 1.42 (t, 3H, *J* = 7.1 Hz)

Elemental analysis:

Calculated: C, 27.50; H, 3.23; N, 0.00; S, 29.37%.

Found: C, 27.56; H, 3.21; N, 0.00; S, 29.73%

L_1Na

White powder obtained with 46% yield.

^{1}H NMR (500 MHz, D_2O, 300 K): δ 4.71 (q, 2H, *J* = 7.1 Hz), 3.83 (s, 2H), 1.43 (t, 3H, *J* = 7.1 Hz)

Elemental analysis:

Calculated: C, 29.70, H, 3.49, N, 0.00, S, 31.71%

Found: C, 29.61, H, 3.48, N, 0.00, S, 32.12%

L_1Li

White powder obtained with a 52% yield.

^{1}H NMR (500 MHz, D_2O, 300 K): δ 4.70 (q, 2H, *J* = 7.1 Hz), 3.81 (s, 2H), 1.42 (t, 3H, *J* = 7.2 Hz)

Elemental analysis:

Calculated: C, 32.26; H, 3.79; N, 0.00, S, 34.45%

Found: C, 31.56; H, 3.62; N, 0.00; S, 34.61%

L_2K

Off-white powder obtained with 30% yield.

^{1}H NMR (500 MHz, D_2O, 300 K): δ 4.70 (qd, 2H, J_q = 7.1 Hz, J_d = 4.8 Hz), 4.27 (q, 1H, *J* = 7.5 Hz), 1.51 (d, 3H, *J* = 7.5 Hz), 1.43 (t, 3H, *J* = 7.2 Hz)

^{13}C NMR (126 MHz, D_2O, 300K): δ 215.2, 178.9, 71.8, 49.8, 16.6, 13.4

Elemental analysis:

Calculated: C, 31.01; H, 3.90; N, 0.00; S, 27.60%

Found: C, 32.23; H, 4.20; N, 0.00; S, 29.05%

Discrepancy attributed to the deliquescence of **L_2K**.

Route b: Benchtop Synthesis of L_1M

As a general example using **L_1K**, in a fumehood, **L_1H** (0.468 g, 2.6 mmol) was dissolved in ethanol (5 mL). Separately, KOH (0.146 g, 2.6 mmol) was dissolved in ethanol (10 mL). The solutions were combined and stirred at room temperature for 45 minutes. The sample was concentrated *in vacuo*, giving a white powder (0.502 g, 88%).

^{1}H NMR (500 MHz, D_2O, 300 K): δ 4.70 (q, 2H, *J* = 7.1 Hz), 3.82 (s, 2H), 1.43 (t, 3H, *J* = 7.1 Hz)

^{13}C NMR (500 MHz, D_2O, 300 K): δ 216.0, 175.4, 71.9, 40.1, 13.5

m/z (ESI-MS): 256.9111 $[L_1K+K]^+$ (calc. 256.9111)

L_1Na

White powder recovered at 80% yield.

^{1}H NMR (500 MHz, D_2O, 300 K): δ 4.70 (q, 2H, *J* = 7.1 Hz), 3.80 (s, 2H), 1.43 (t, 3H, *J* = 7.1 Hz)

^{13}C NMR (500 MHz, D_2O, 300 K): δ 216.3, 175.8, 71.9, 40.4, 13.5

m/z (ESI-MS): 224.9622 $[L_1Na+Na]^+$ (calc. 224.9627)

L_1Li

The general method was slightly modified due to the limited solubility of LiOH, which was instead dissolved in a solution of ethanol (4 mL) and deionised water (1 mL).

White powder obtained with 88% yield.

^{1}H NMR (500 MHz, D_2O, 300 K): δ 4.70 (q, 2H, *J* = 7.2 Hz), 3.78 (s, 2H), 1.42 (t, 3H, *J* = 7.2 Hz)

^{13}C NMR (126 MHz, D_2O, 300 K): δ 216.3, 175.8, 71.9, 40.4, 13.5

m/z (ESI-MS): 193.0151 $[L_1Li+Li]^+$ (calc. 193.0157)

General Ring-opening Copolymerisation Procedure

In a glovebox (or fumehood for "benchtop conditions"), **L_1K** (7.6 mg, 0.035 mmol), phthalic anhydride (518.4 mg, 3.5 mmol) and cyclohexene oxide (1.4 mL, 14 mmol) were added to a vial equipped with a stirrer bar. The vial was sealed and placed in a 100 °C for the desired amount of time, then quenched with chloroform. An aliquot was taken for NMR ($CDCl_3$), and the remainder was dissolved in chloroform and precipitated in cold methanol.

General Block Copolymerisation Procedure

In a fumehood, vinyl acetate was passed through basic alumina and sparged with argon for 30 minutes. Polyester (0.01 mmol, based on the molecular weight from SEC analysis), AIBN (40 µL of 10 mg mL^{-1} solution in vinyl acetate), vinyl acetate (330 µL, in total 4 mmol) were added to a vial. The solution was further sparged for 5 minutes before sealing and placing in a 65 °C aluminium heating block for the desired amount of time. The polymerisation was quenched by cooling the reaction and opening the vial to expose it to air. An aliquot was taken for NMR analysis in $CDCl_3$ solvent. The remainder was dissolved in THF and precipitated in cold pentane. If desired, the resultant copolymer product could be purified by stirring the reaction mixture in cold methanol, and removing the insoluble homo-polyester by filtration. Subsequent removal of the methanol solvent from the filtrate, by using compressed air, gave the block copolymer.

Characterisation data for L_1H

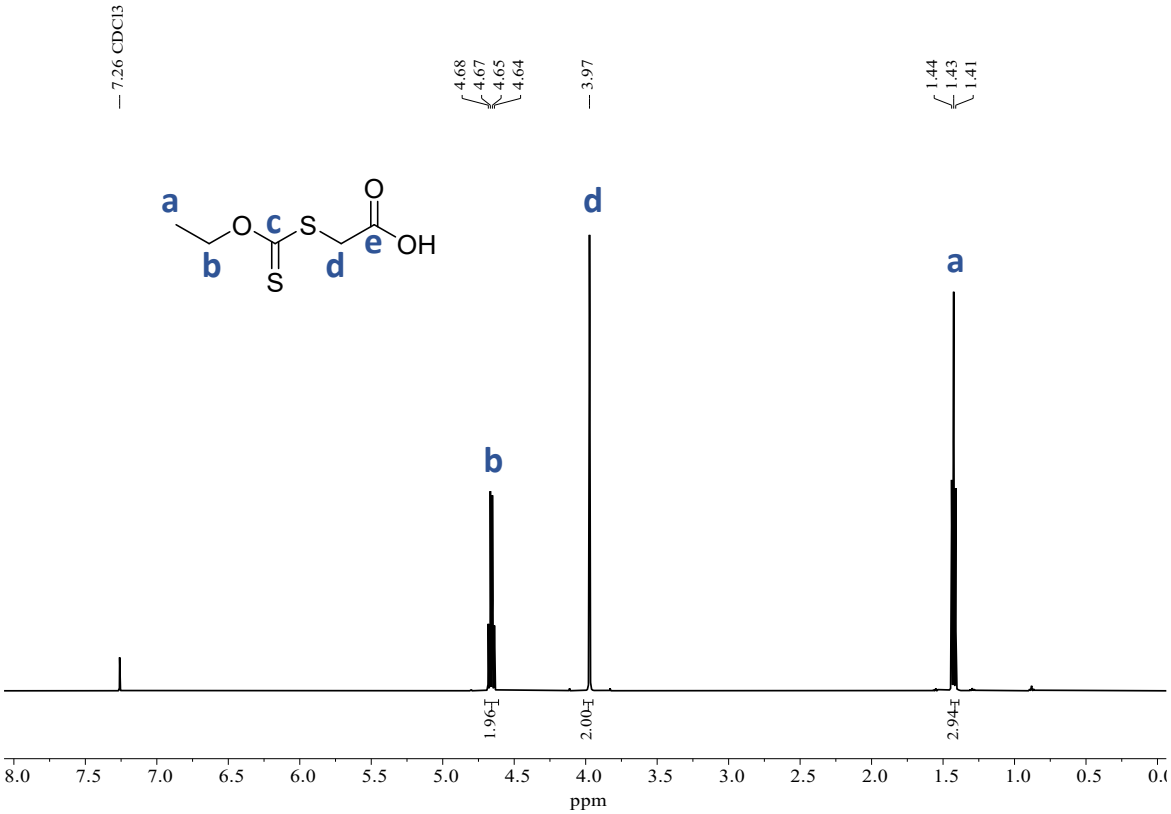

Figure S1: ^{1}H NMR spectrum of **L_1H** in $CDCl_3$ (300 K).

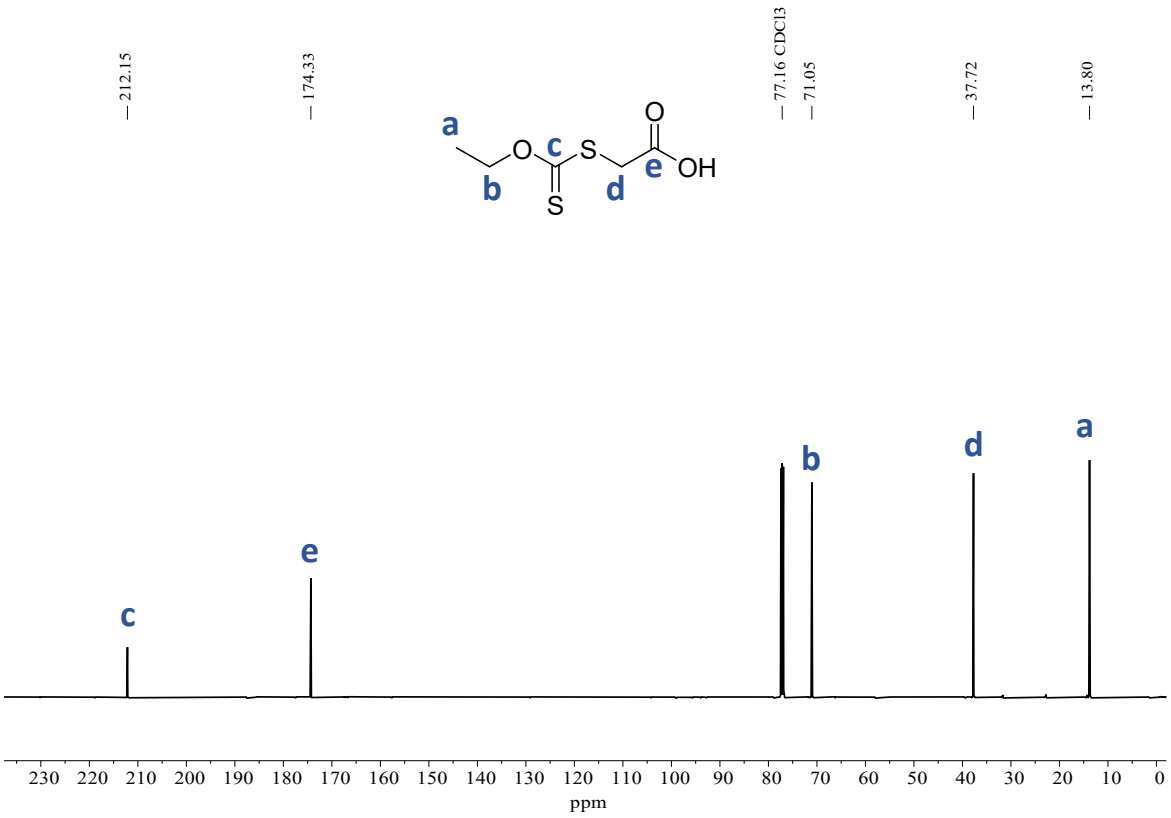

Figure S2: ^{13}C NMR spectrum of **L_1H** in $CDCl_3$.

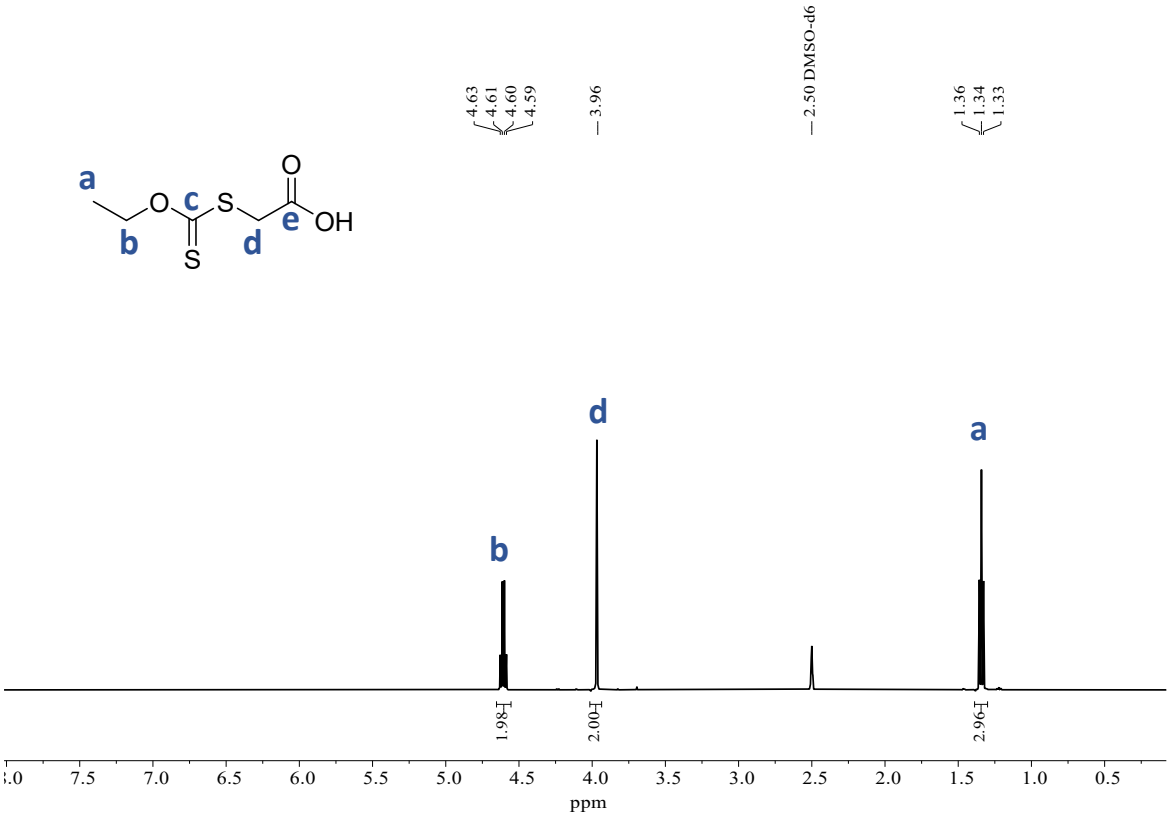

Figure S3: ^{1}H NMR spectrum of **L_1H** in DMSO-d_6 (300 K).

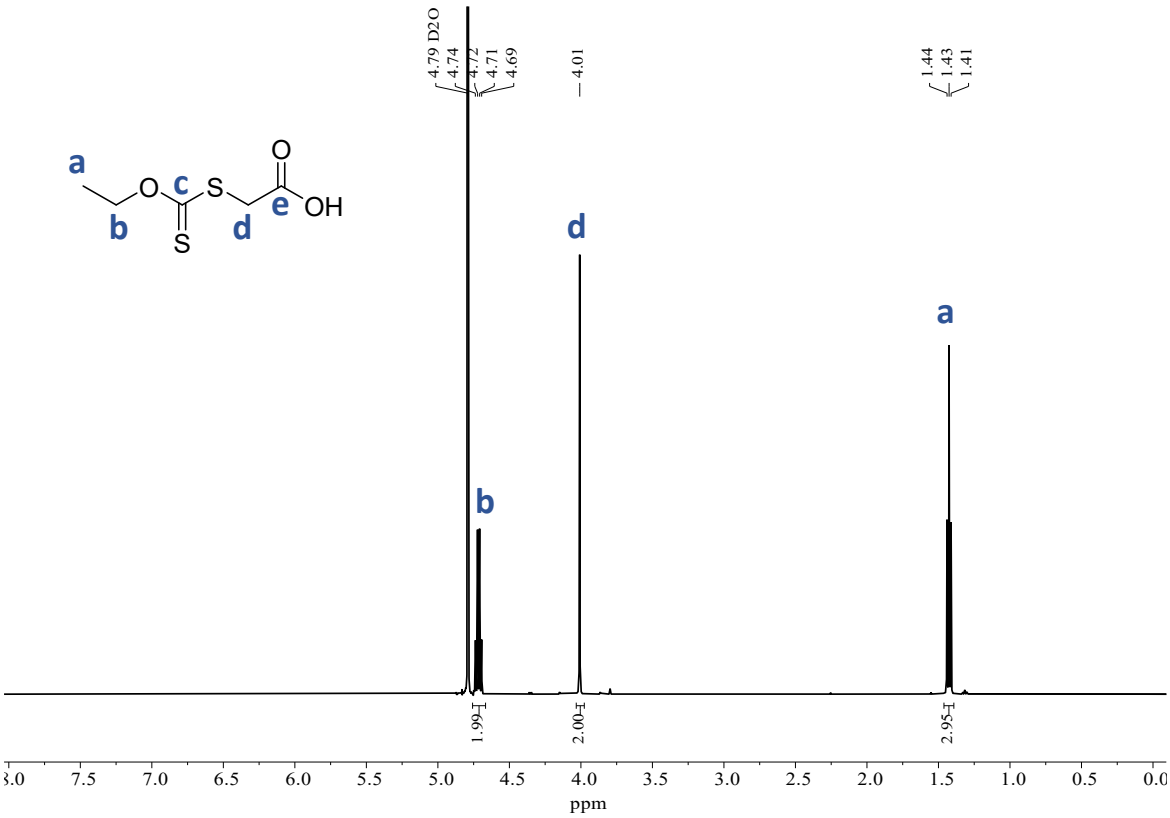

Figure S4: ^{1}H NMR spectrum **L_1H** in D_2O (300 K).

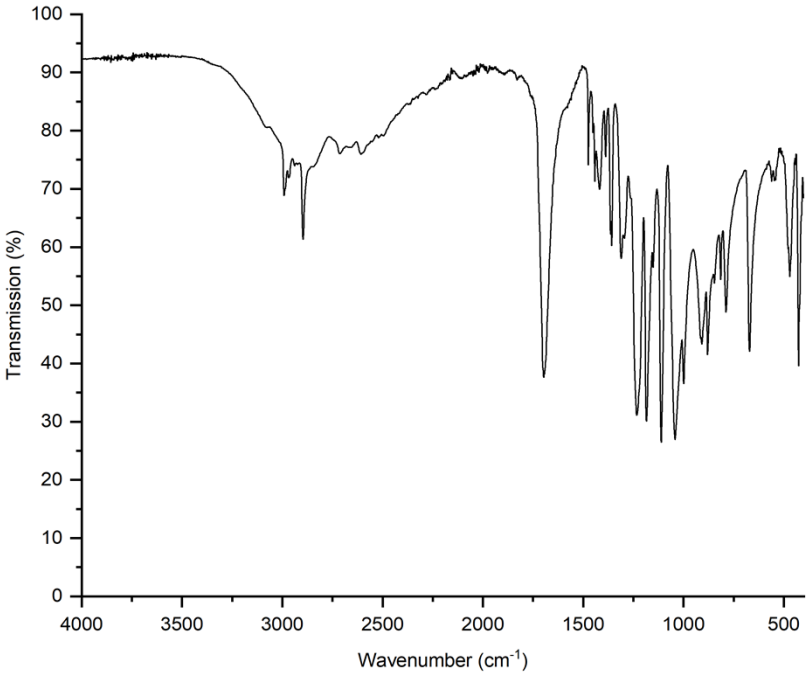

Figure S5: IR spectrum of **L_1H**.

Characterisation data for L_2H

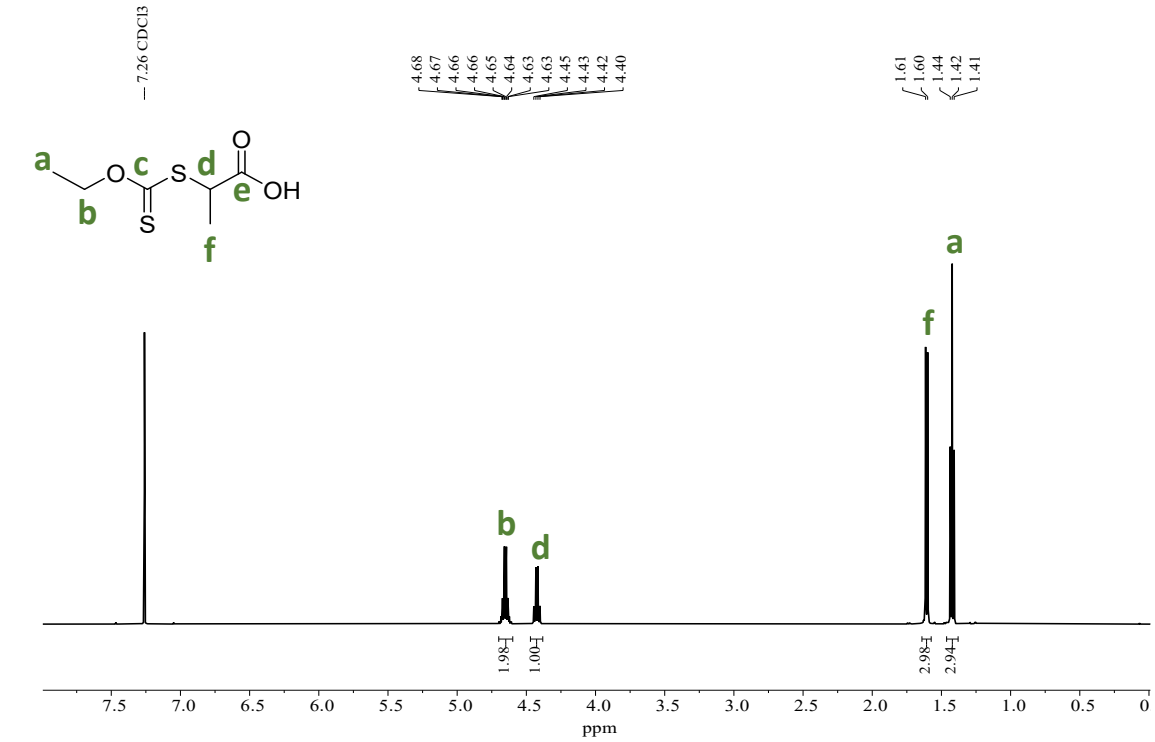

Figure S6: ^{1}H NMR spectrum of **L_2H** in $CDCl_3$ (300 K).

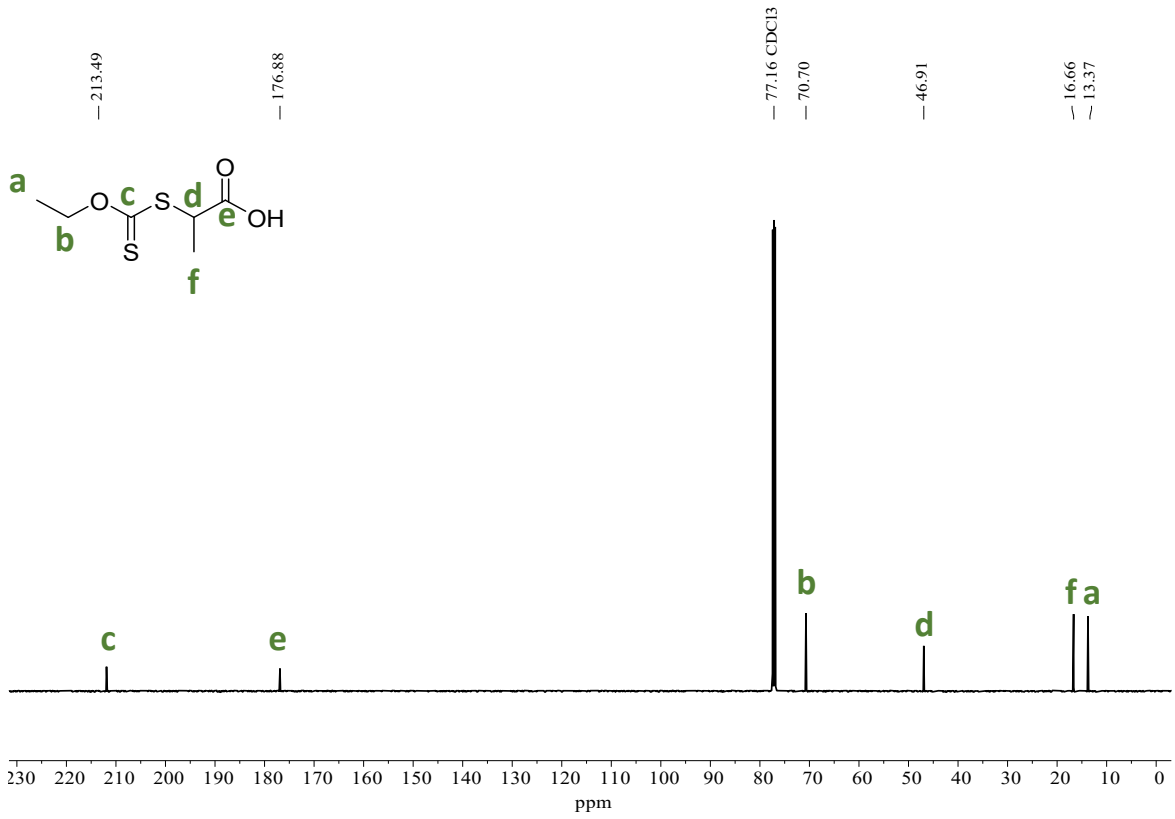

Figure S7: ^{13}C NMR spectrum of **L_2H** in $CDCl_3$ (300 K).

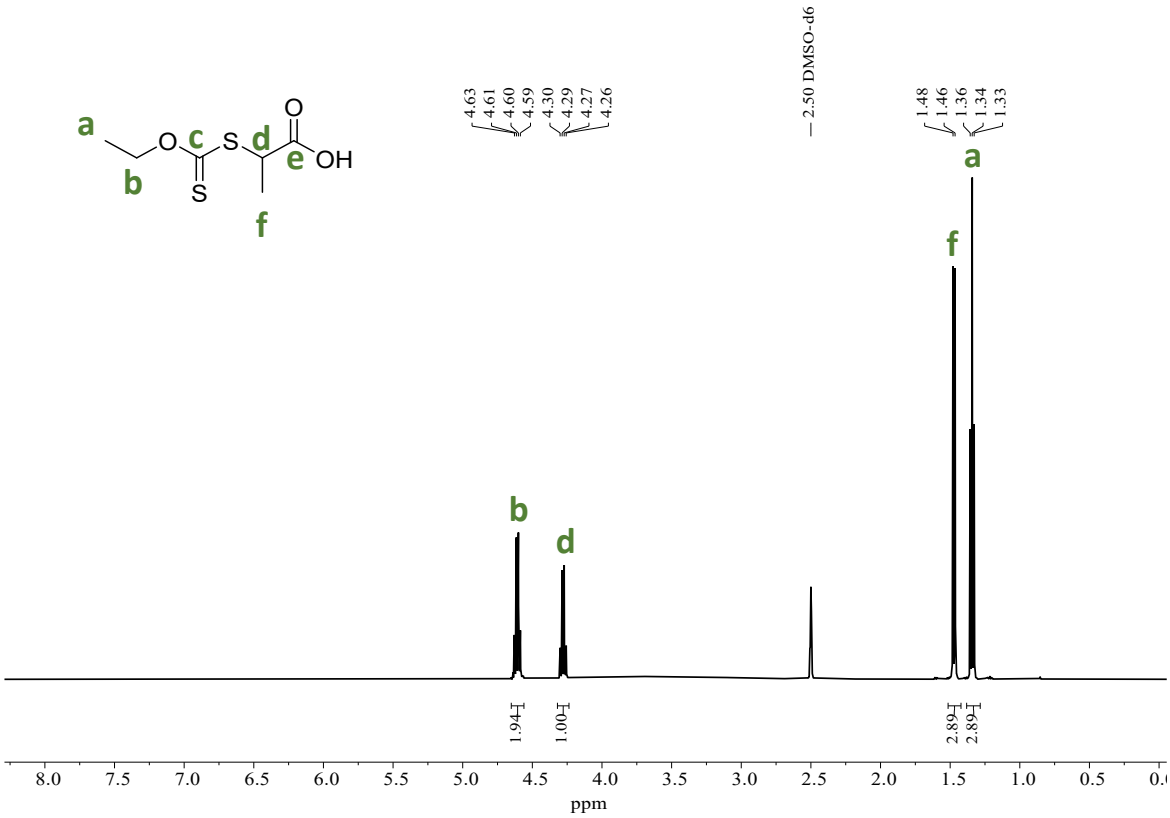

Figure S8: ^{1}H NMR of **L_2H** in DMSO-d_6 (300 K).

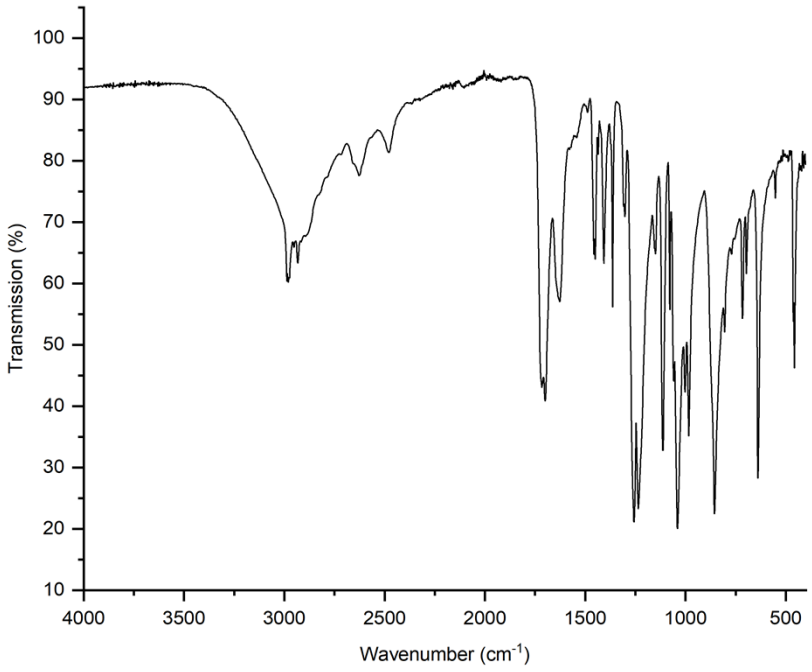

Figure S9: IR spectrum of **L_2H**.

Characterisation data for L_1Li

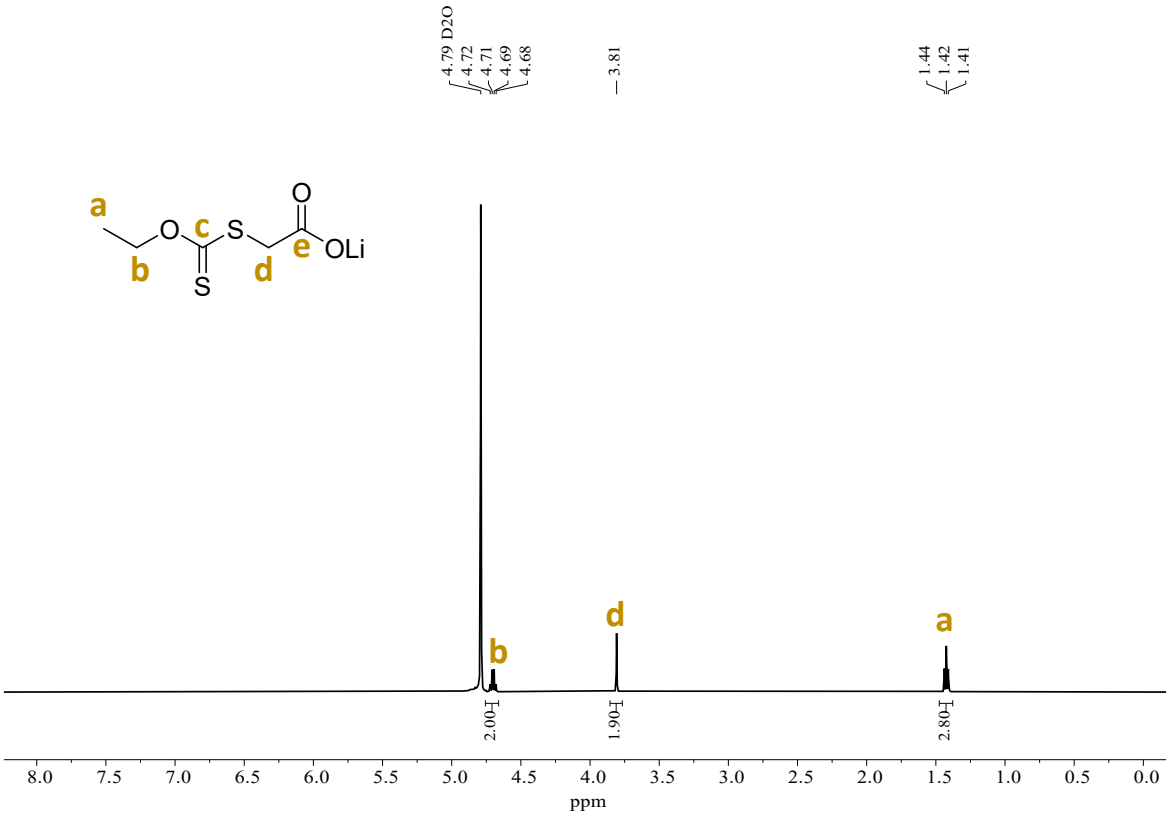

Figure S10: ^{1}H NMR spectrum of **L_1Li** (glovebox synthesis) in D_2O (300 K).

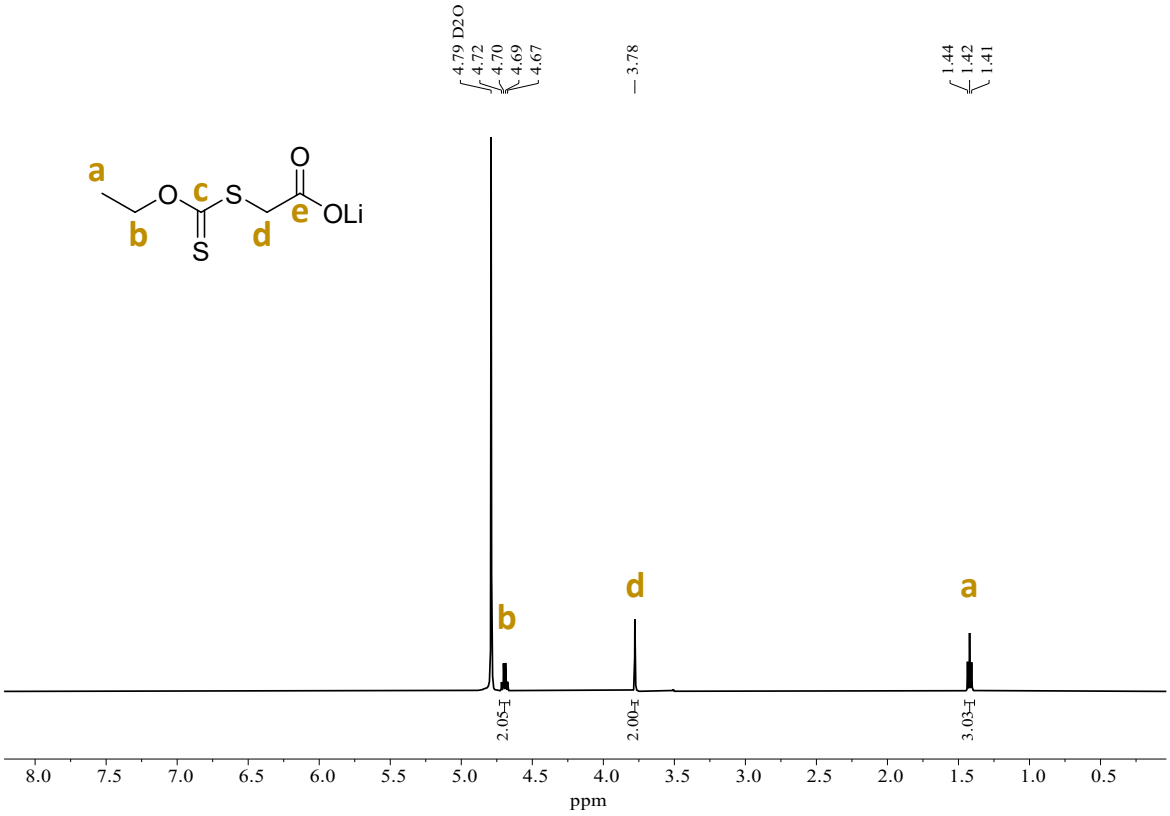

Figure S11: ^{1}H NMR spectrum of **L_1Li** (benchtop synthesis) in D_2O (300 K).

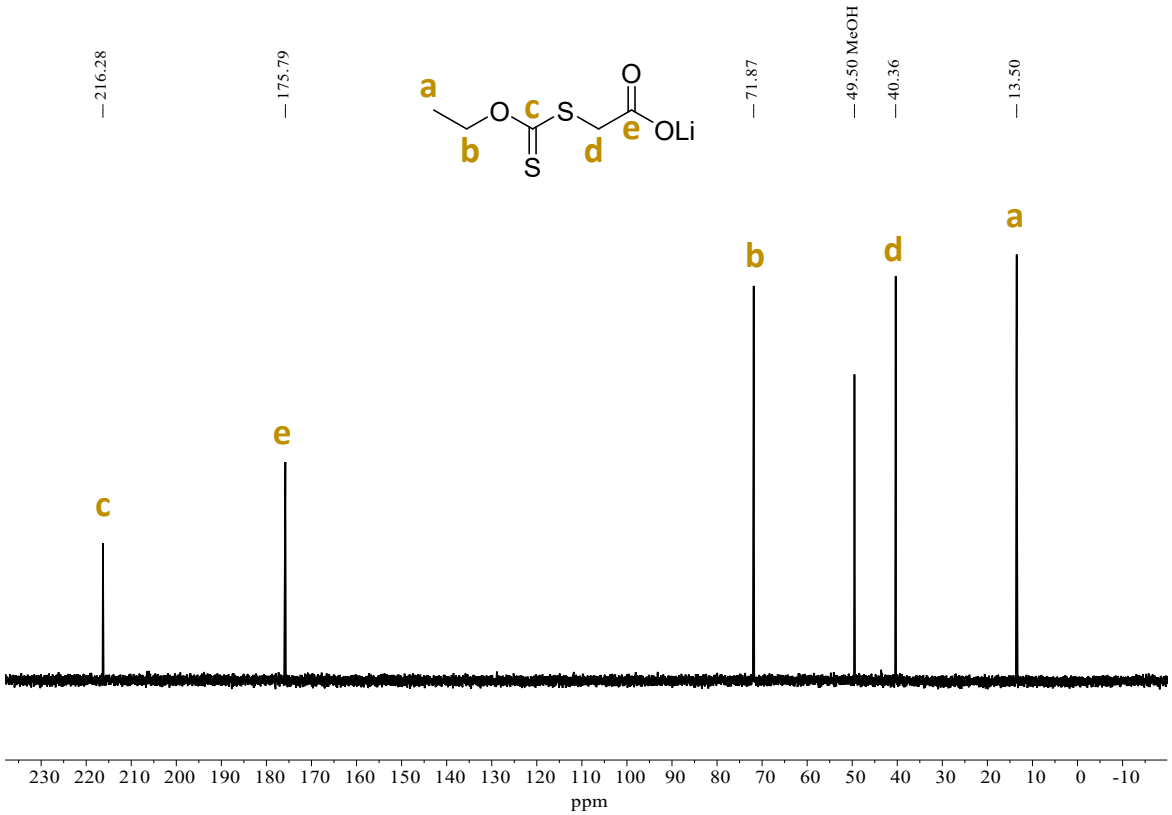

Figure S12: ^{13}C NMR spectrum of **L_1Li** (benchtop synthesis) in D_2O (300 K).

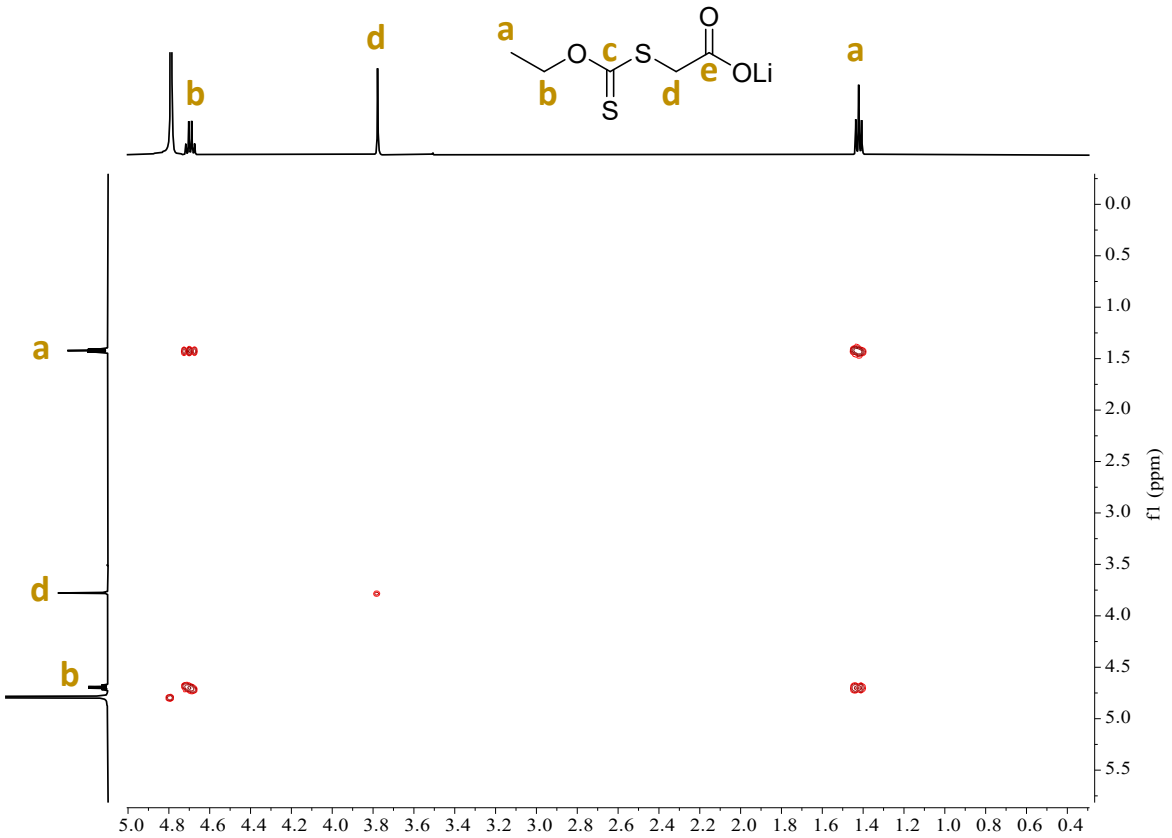

Figure S13: COSY NMR spectrum of **L_1Li** (benchtop synthesis) in D_2O (300 K).

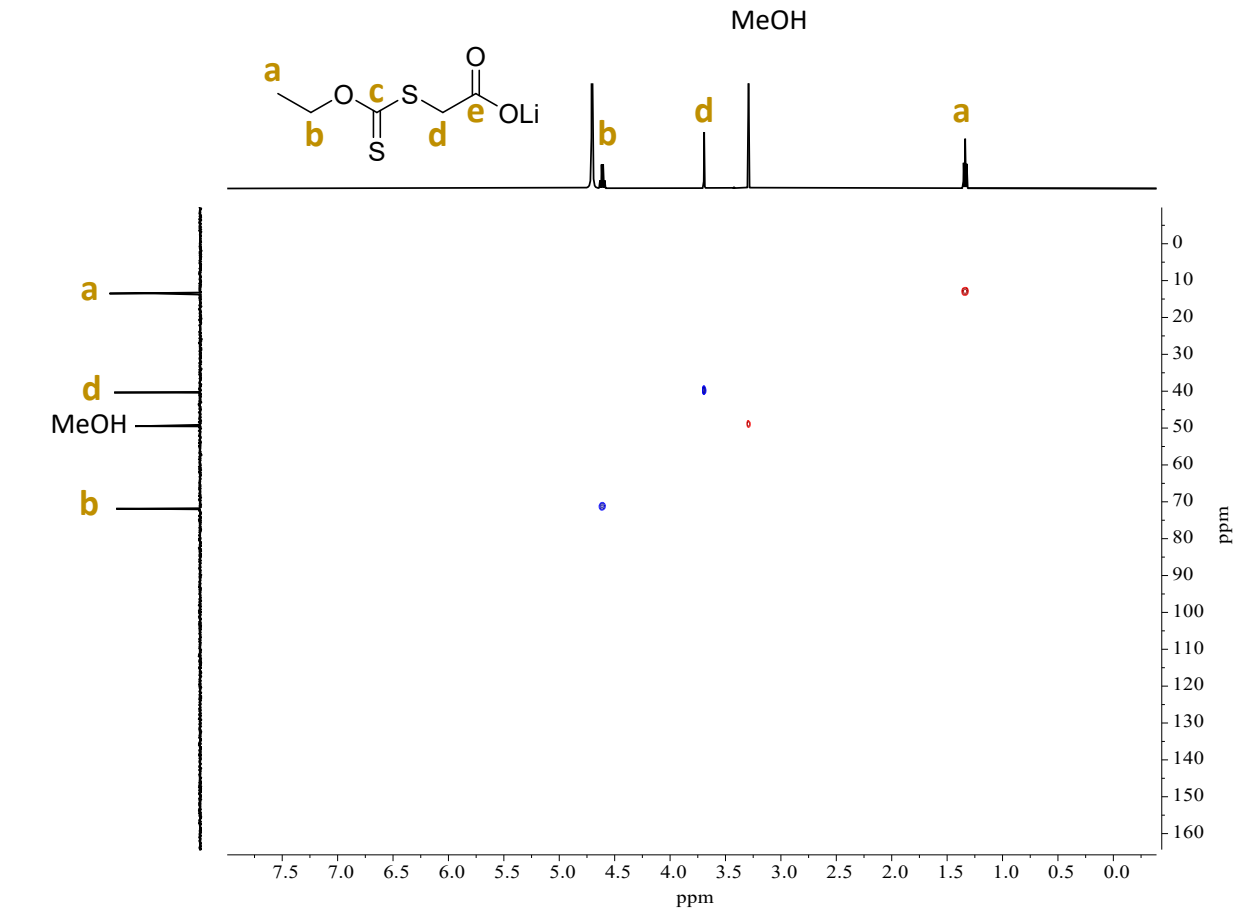

Figure S14: HSQC NMR spectrum of **L_1Li** (benchtop synthesis) in D_2O (300 K).

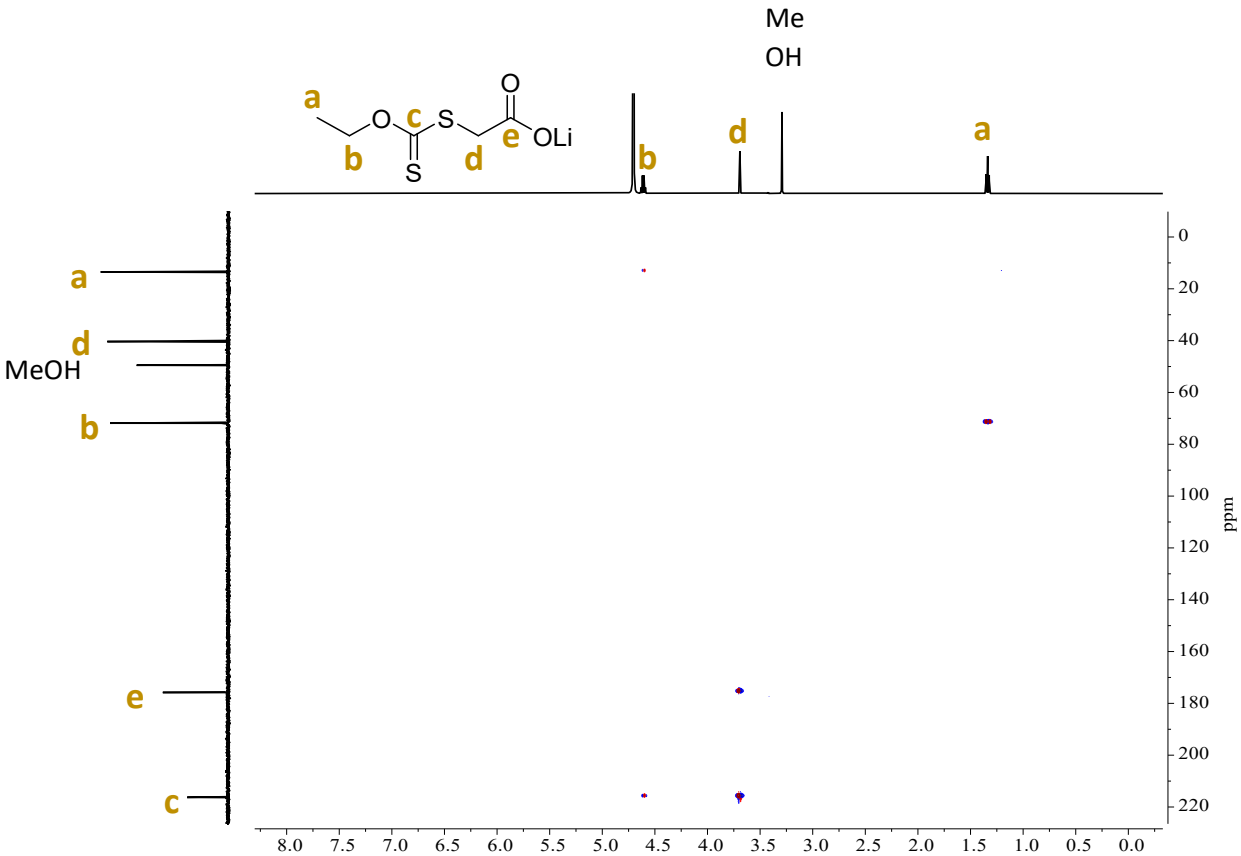

Figure S15: HMBC NMR spectrum of **L_1Li** (benchtop synthesis) in D_2O (300 K).

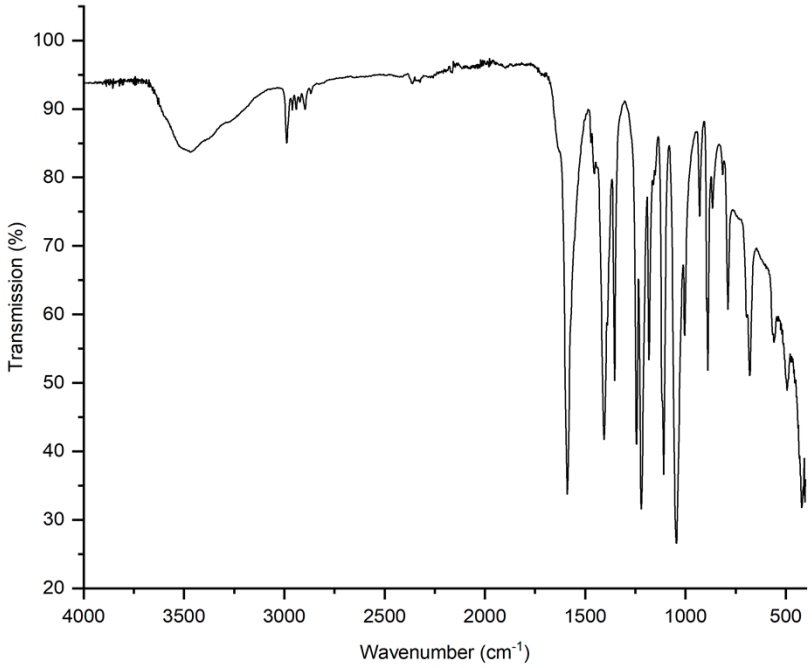

Figure S16: IR spectrum of **L_1Li** (benchtop synthesis).

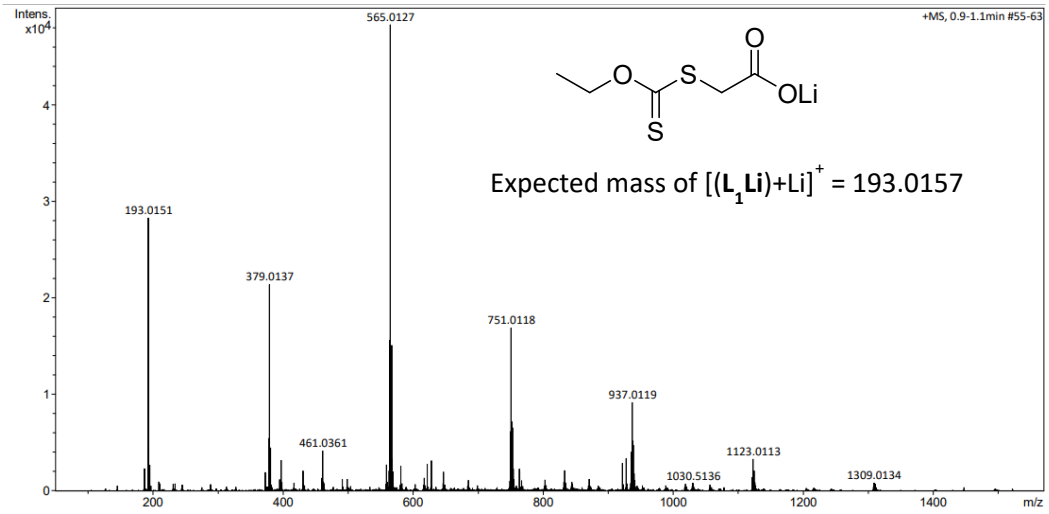

Figure S17: ESI-MS spectrum of **L_1Li** (benchtop synthesis).

Characterisation data for L_1Na

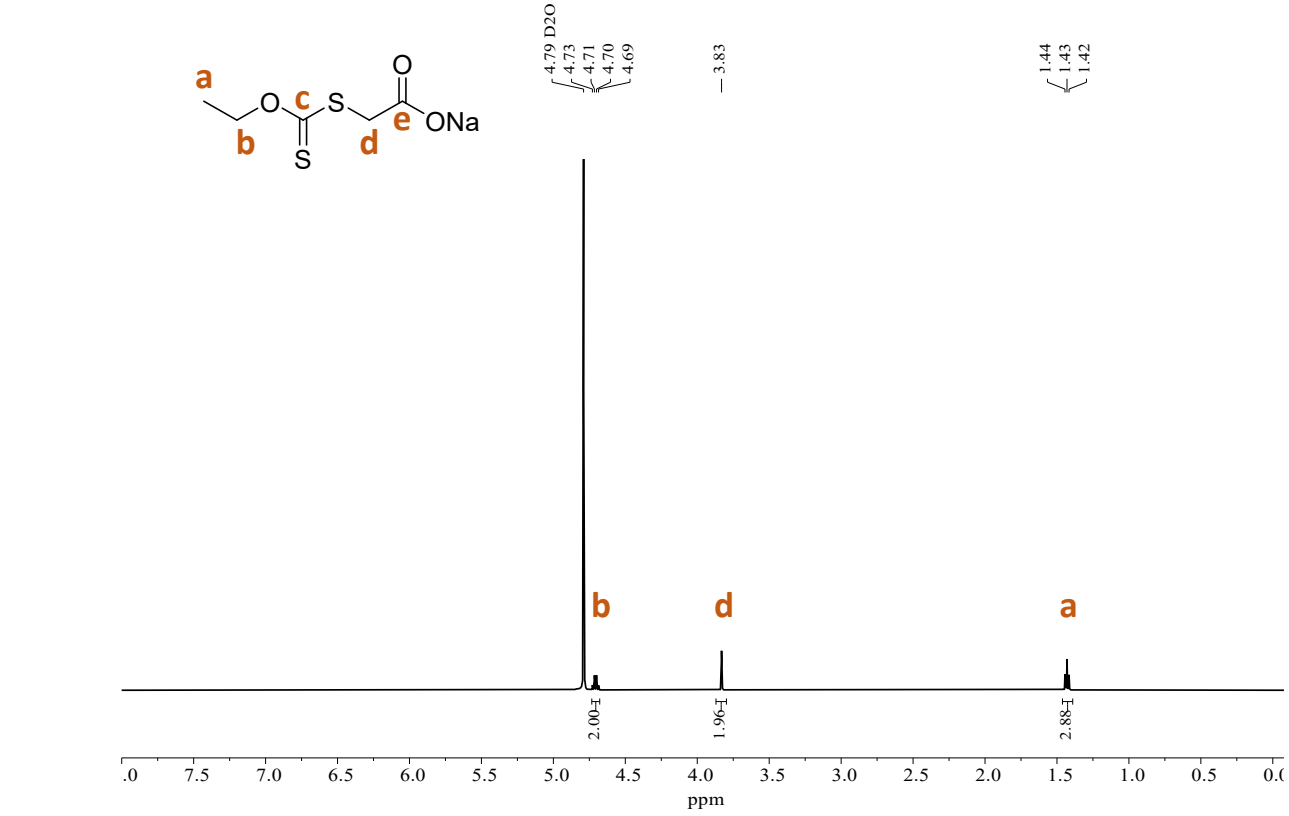

Figure S18 ^{1}H NMR spectrum of **L_1Na** (glovebox synthesis) in D_2O (300 K).

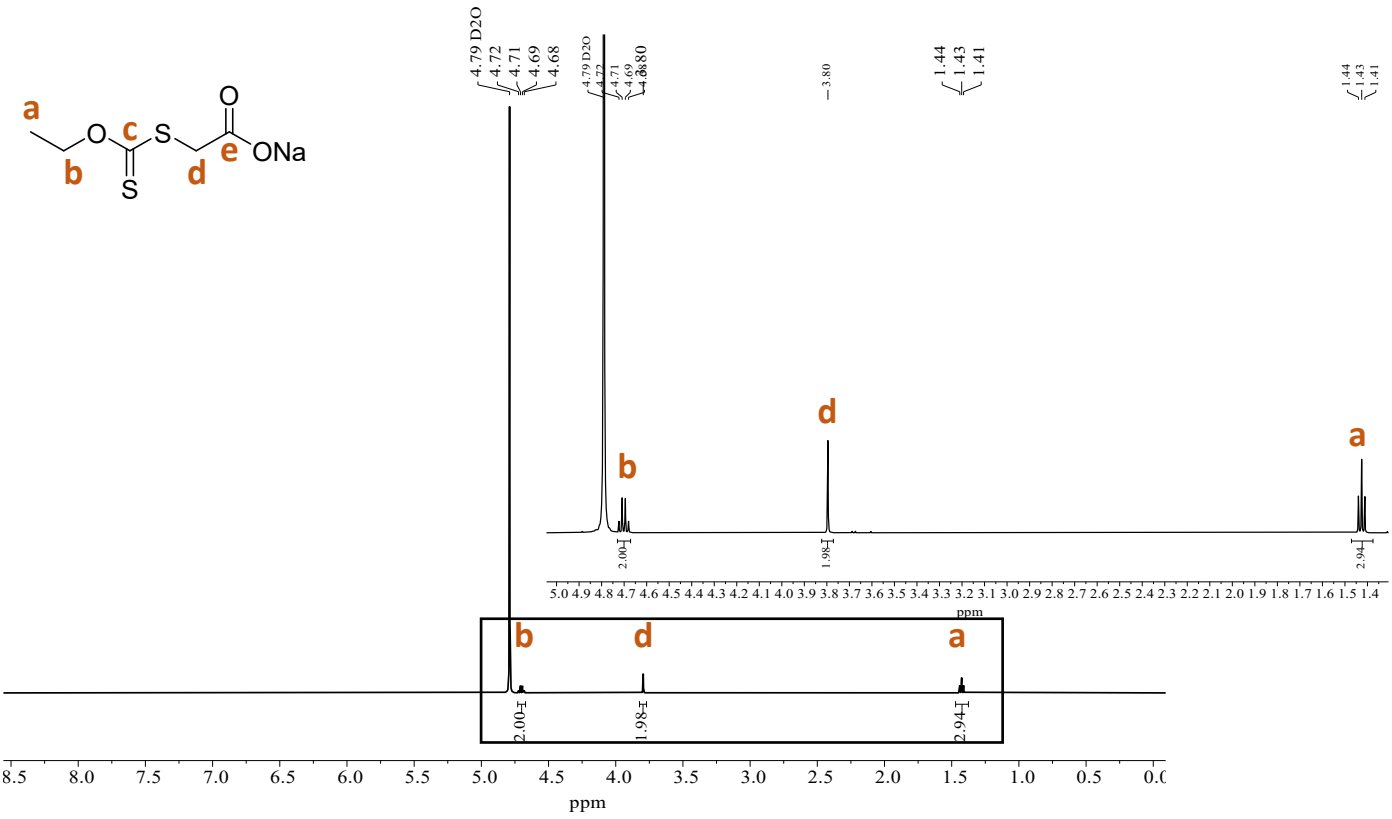

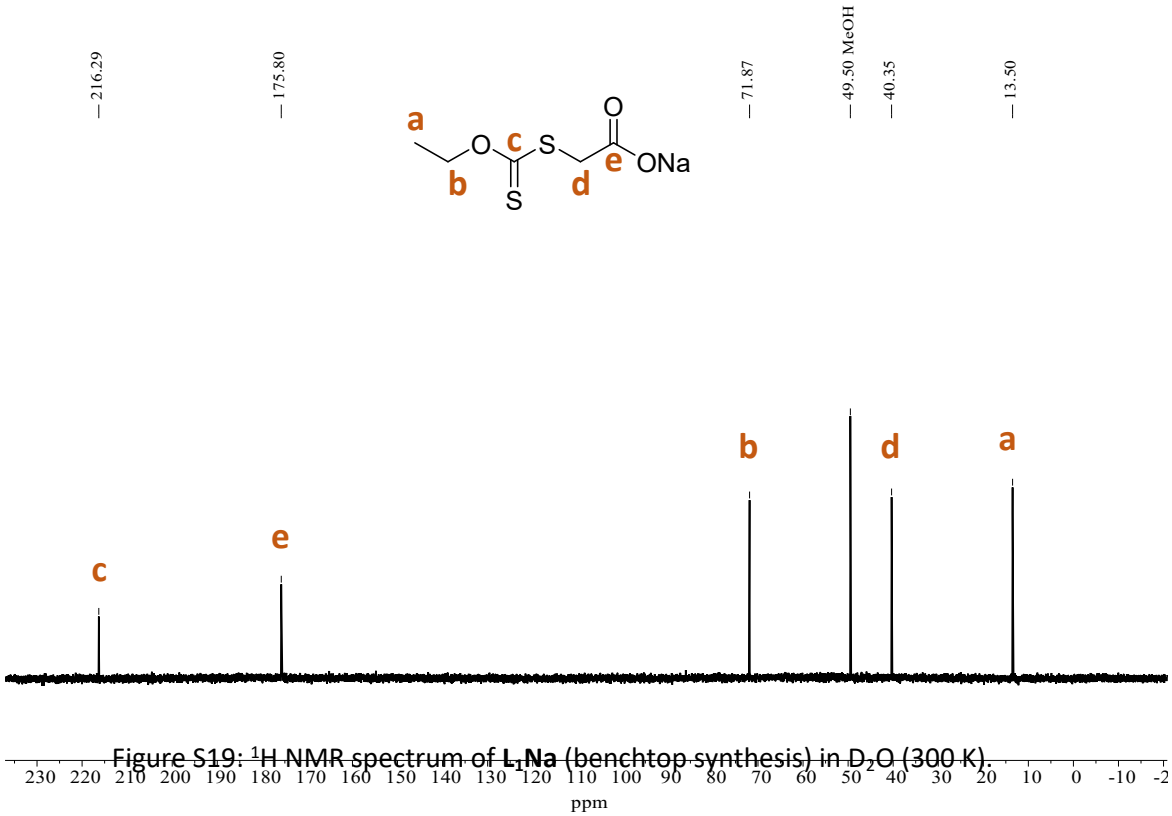

Figure S19: ^{1}H NMR spectrum of **L_1Na** (benchtop synthesis) in D_2O (300 K).

Figure S20: ^{13}C NMR spectrum of **L_1Na** (benchtop synthesis) in D_2O (300 K).

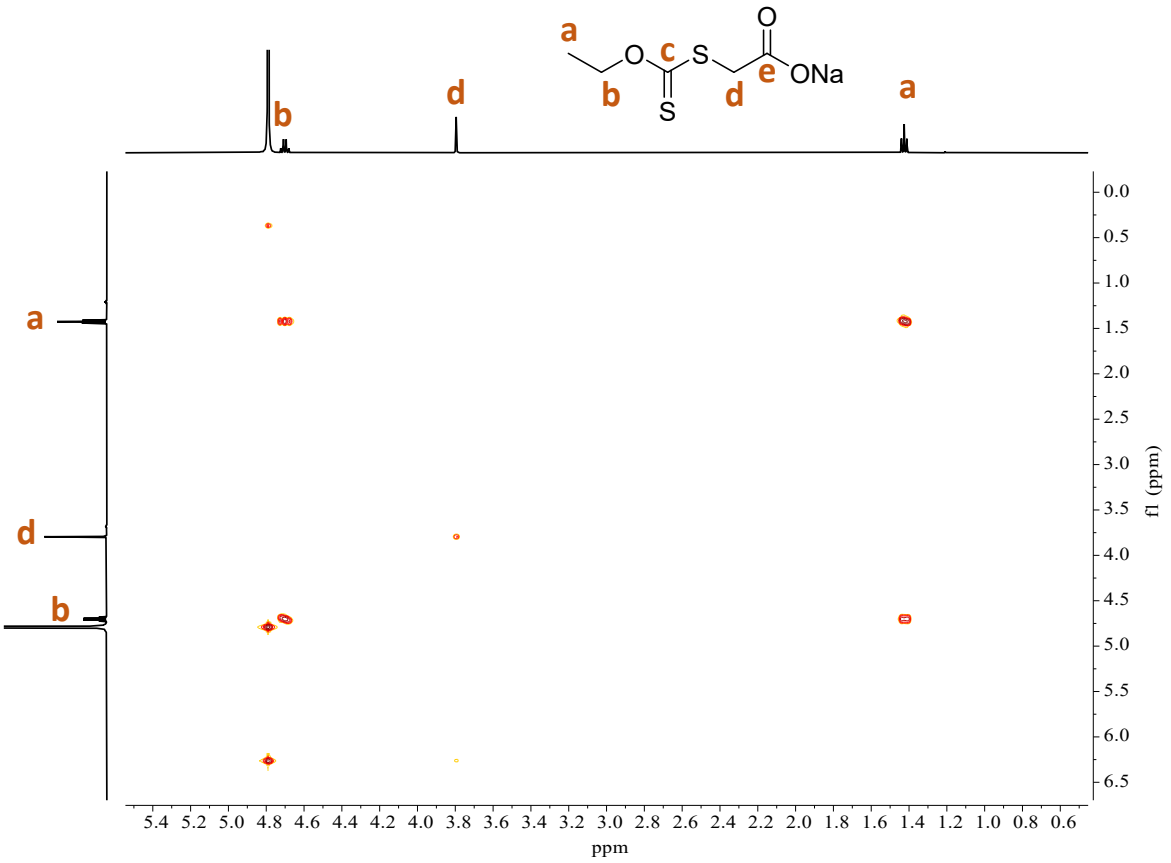

Figure S21: COSY NMR spectrum of **L_1Na** (benchtop synthesis) in D_2O (300 K).

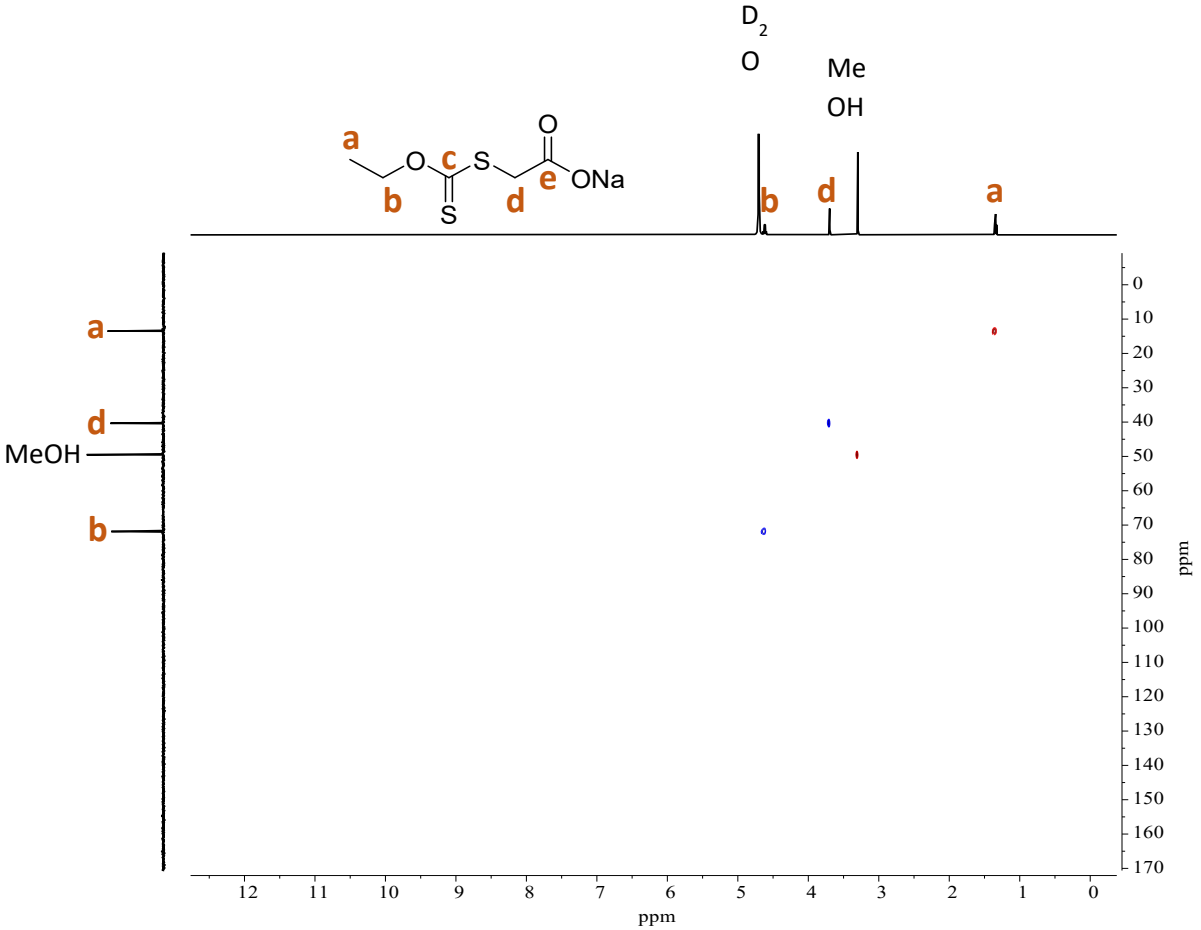

Figure S22: HSQC NMR spectrum of **L_1Na** (benchtop synthesis) in D_2O (300 K).

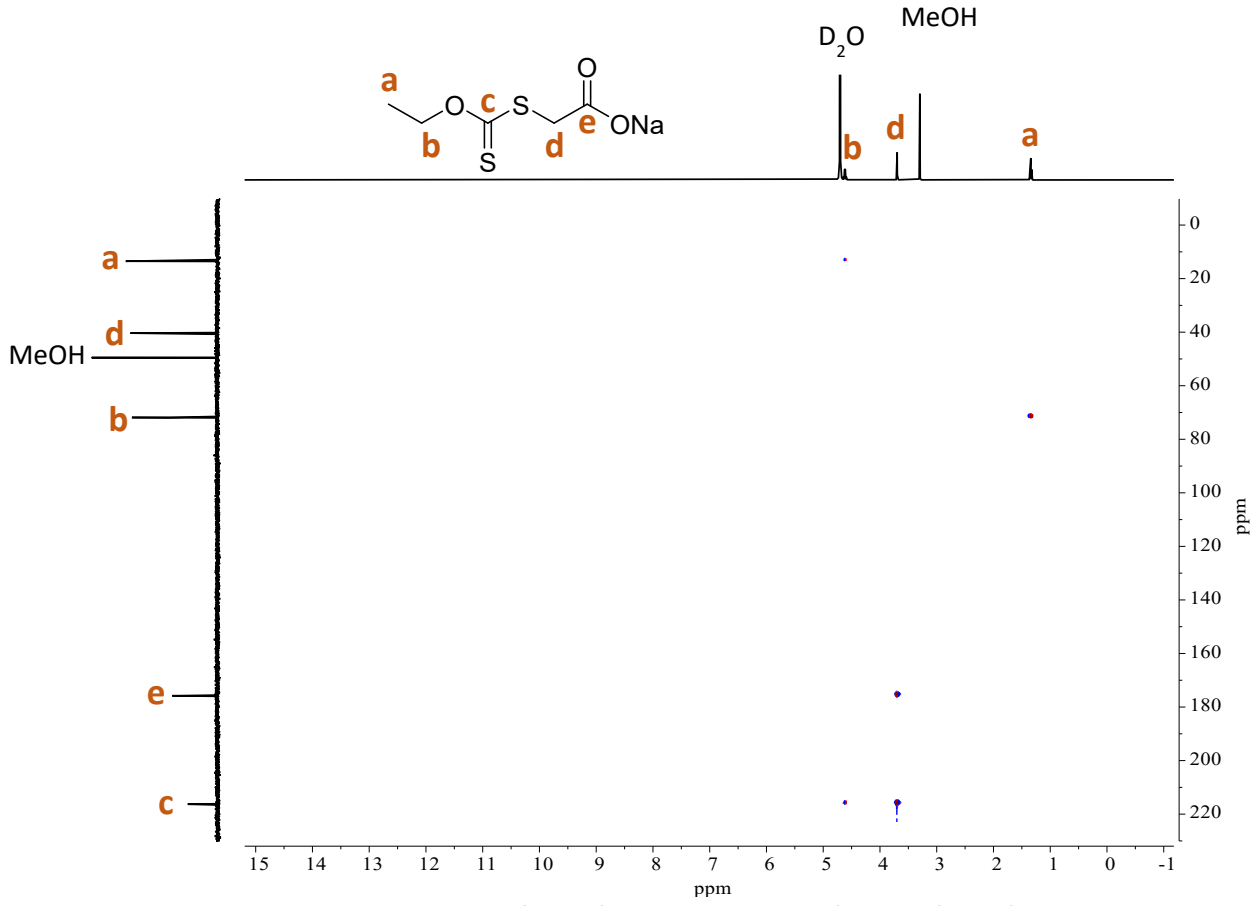

Figure S23: HMBC NMR spectrum of **L_1Na** (benchtop synthesis) in D_2O (300 K).

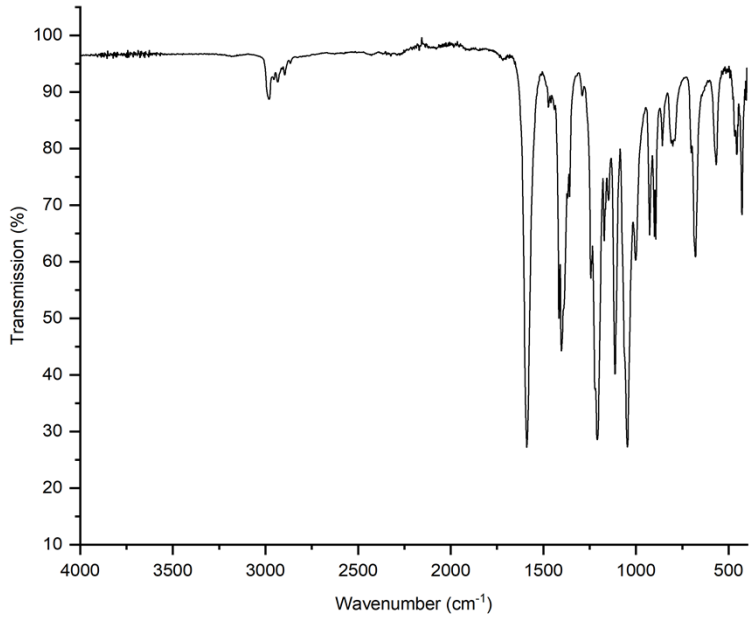

Figure S24: IR spectrum of **L_1Na** (benchtop synthesis).

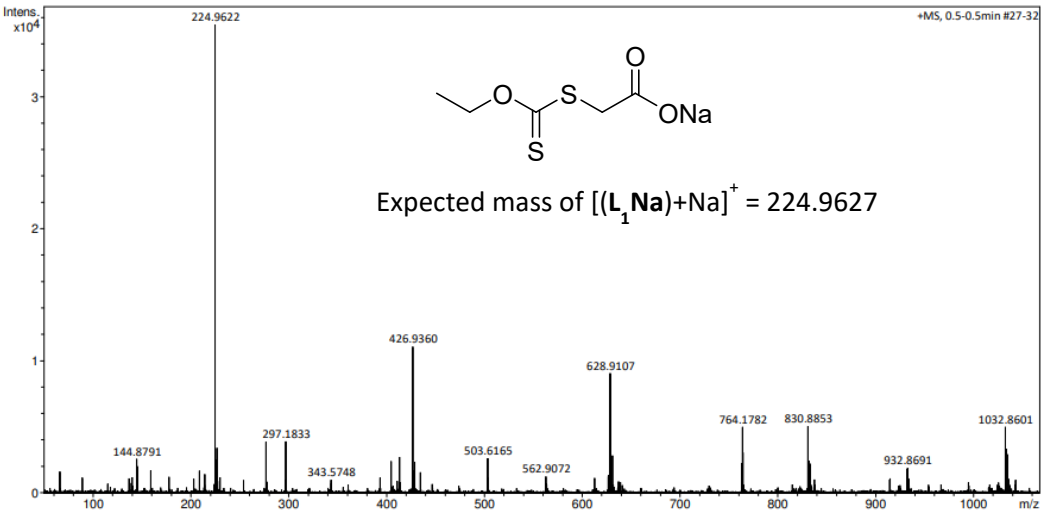

Figure S25: ESI-MS of **L_1Na** (benchtop synthesis).

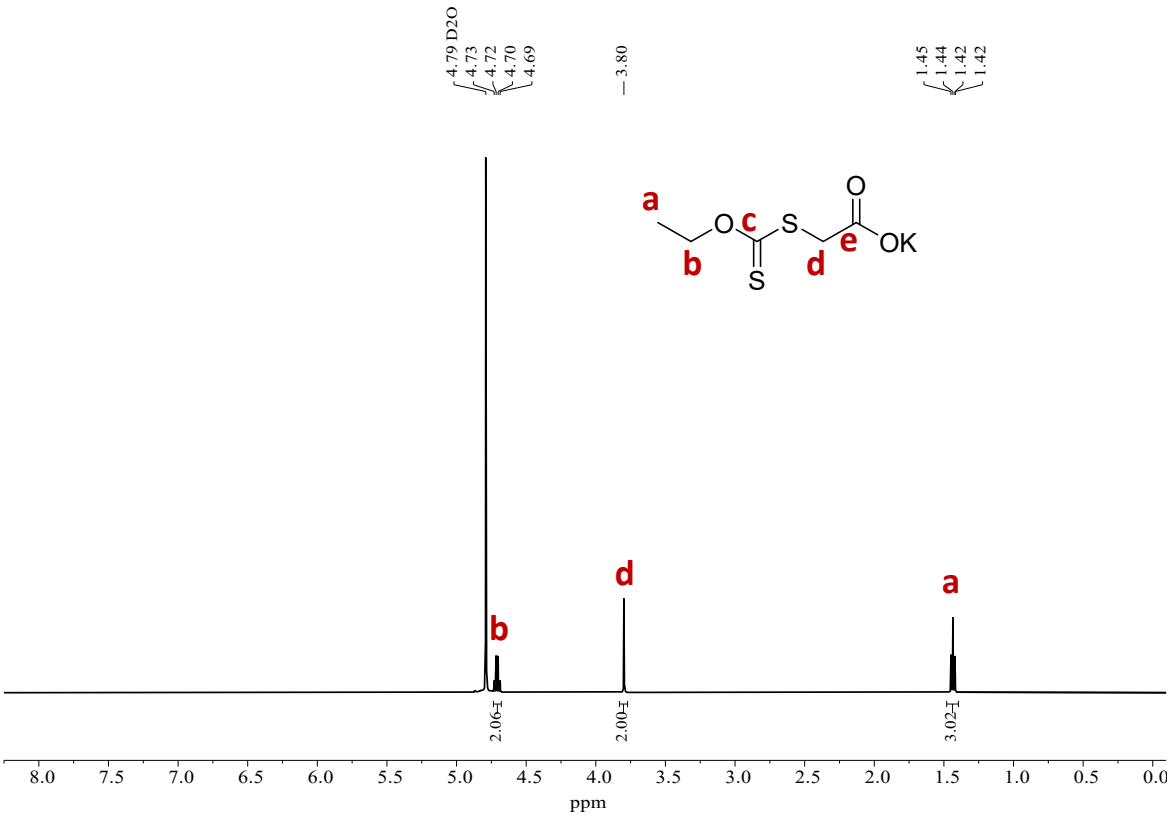

Figure S26: ^{1}H NMR spectrum of **L_1K** (air-sensitive synthesis) in D_2O (300 K).

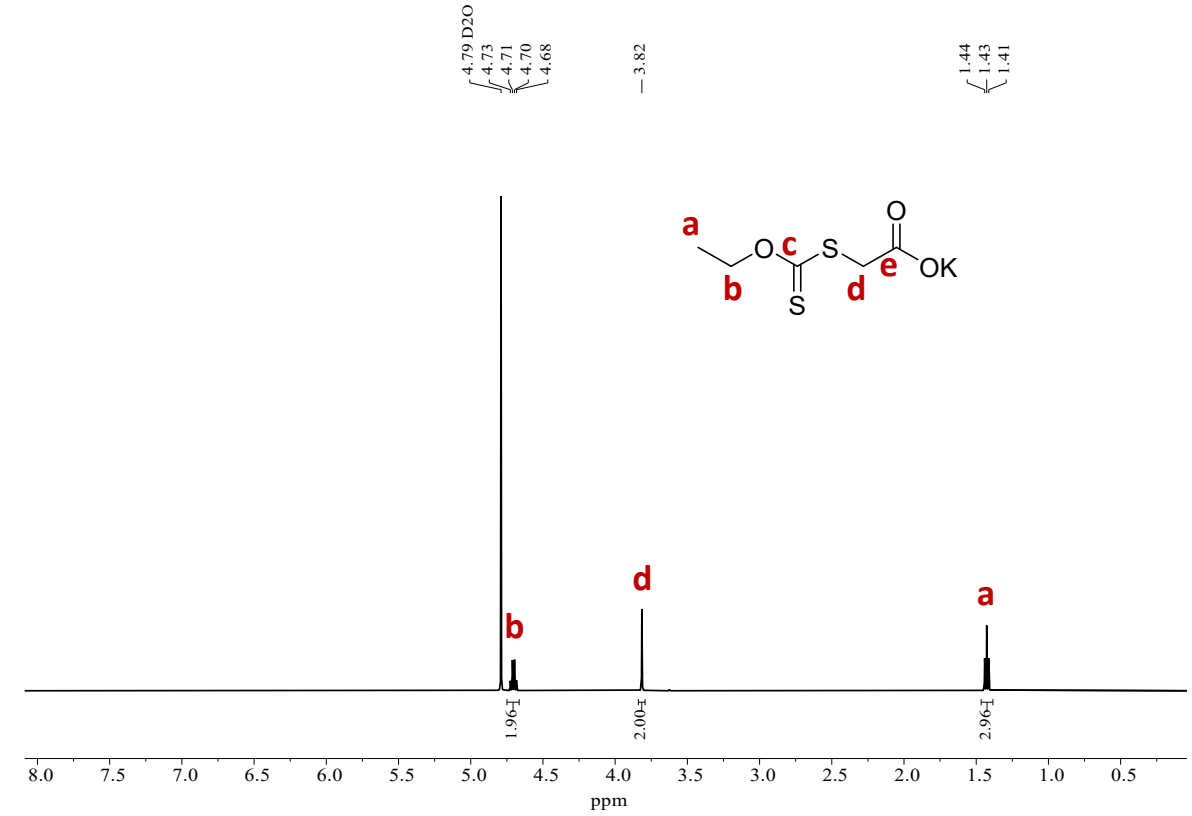

Characterisation data for L_1K

Figure S27: ^{1}H NMR spectrum of **L_1K** (benchtop synthesis) in D_2O (300 K).

Figure S28: ^{13}C NMR spectrum of **L_1K** (benchtop synthesis) in D_2O (300 K).

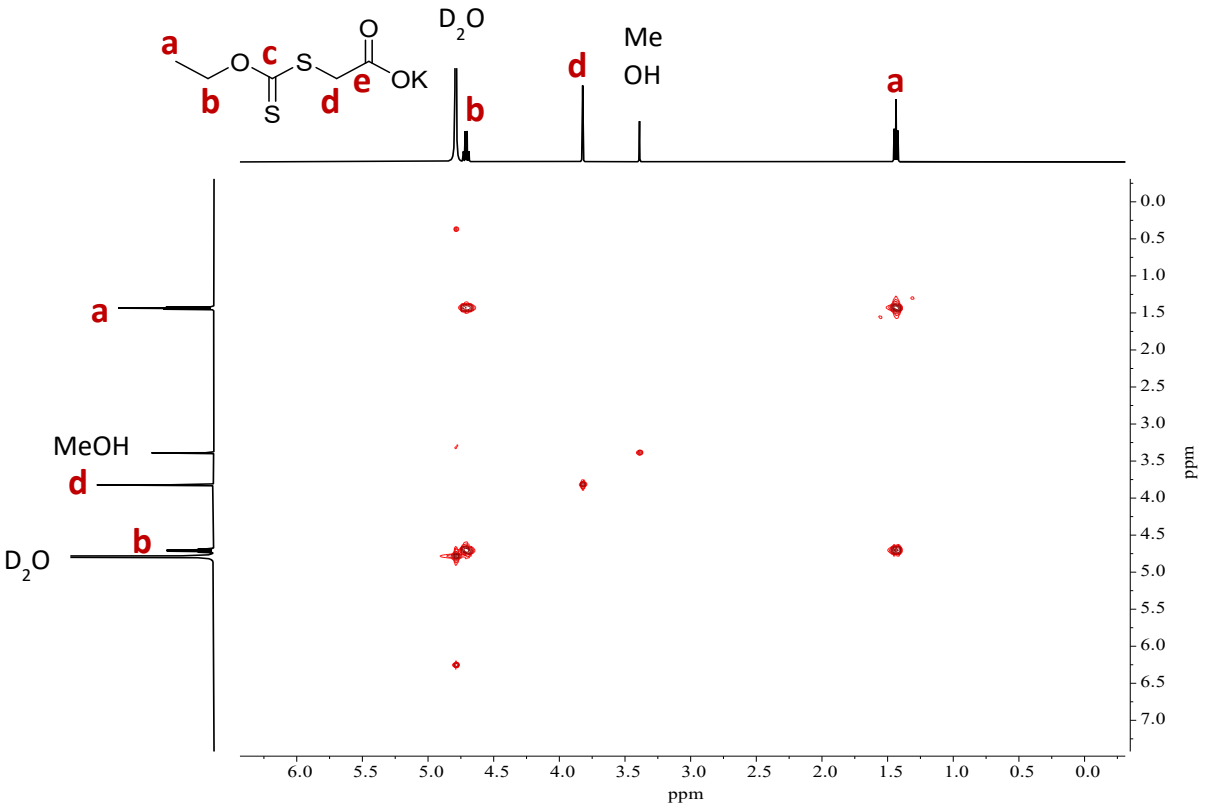

Figure S29: COSY NMR spectrum of **L_1K** (benchtop synthesis) in D_2O (300 K).

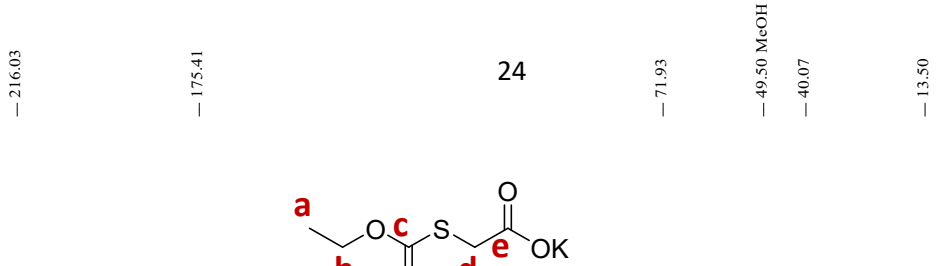

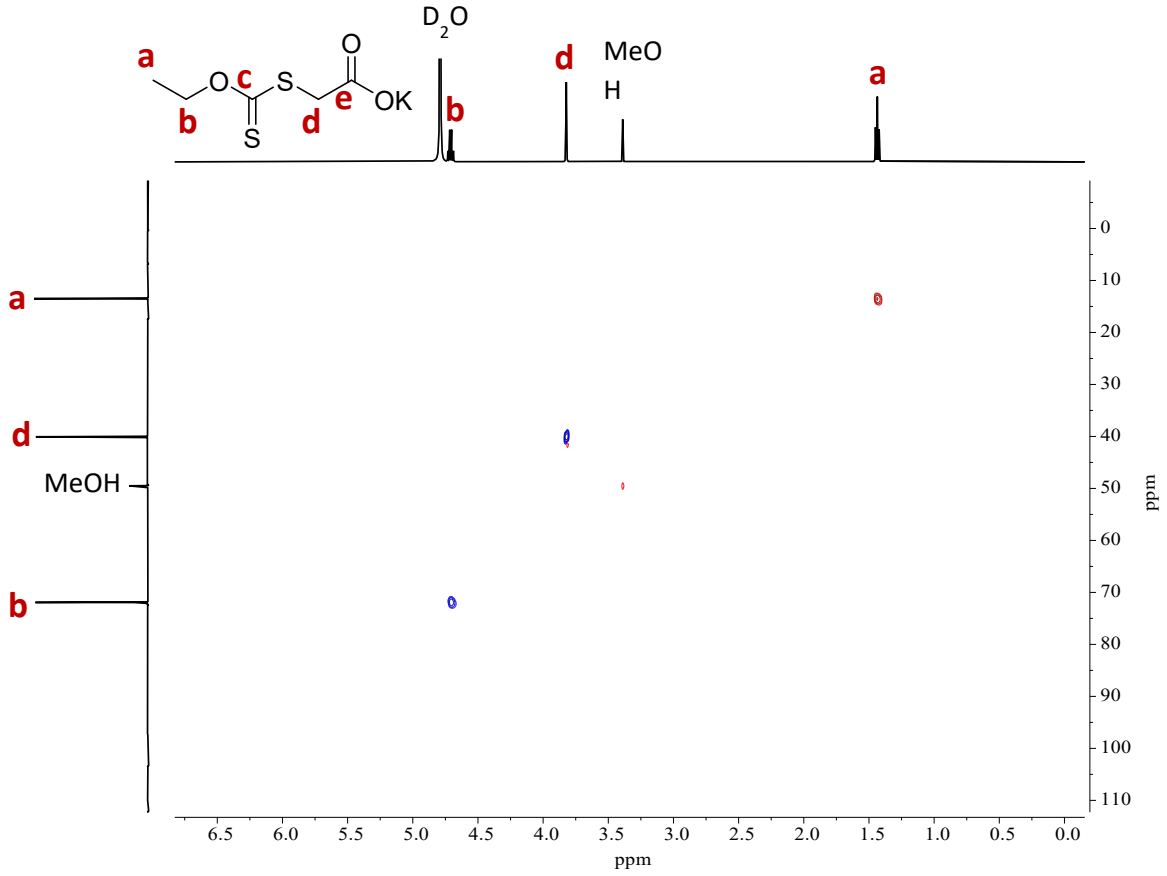

Figure S30: HSQC NMR spectrum of **L_1K** (benchtop synthesis) in D_2O (300 K).

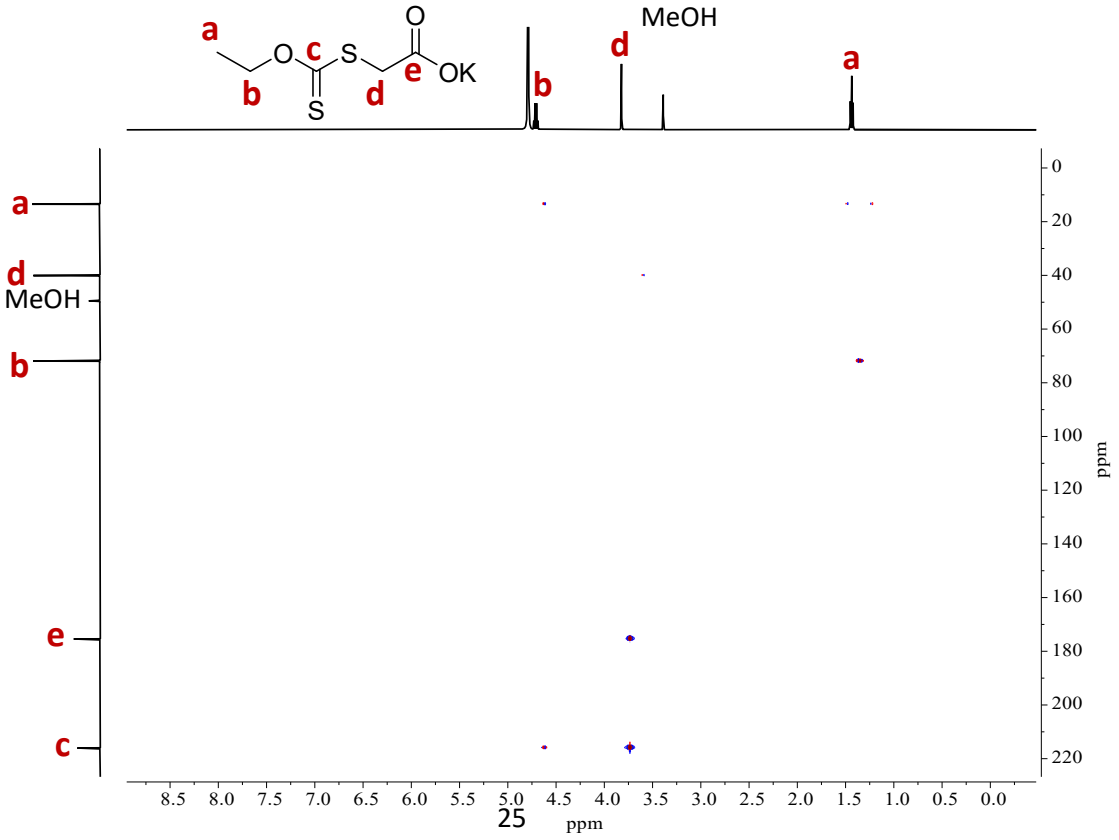

Figure S31: HMBC NMR spectrum of **L_1K** (benchtop synthesis) in D_2O (300 K).

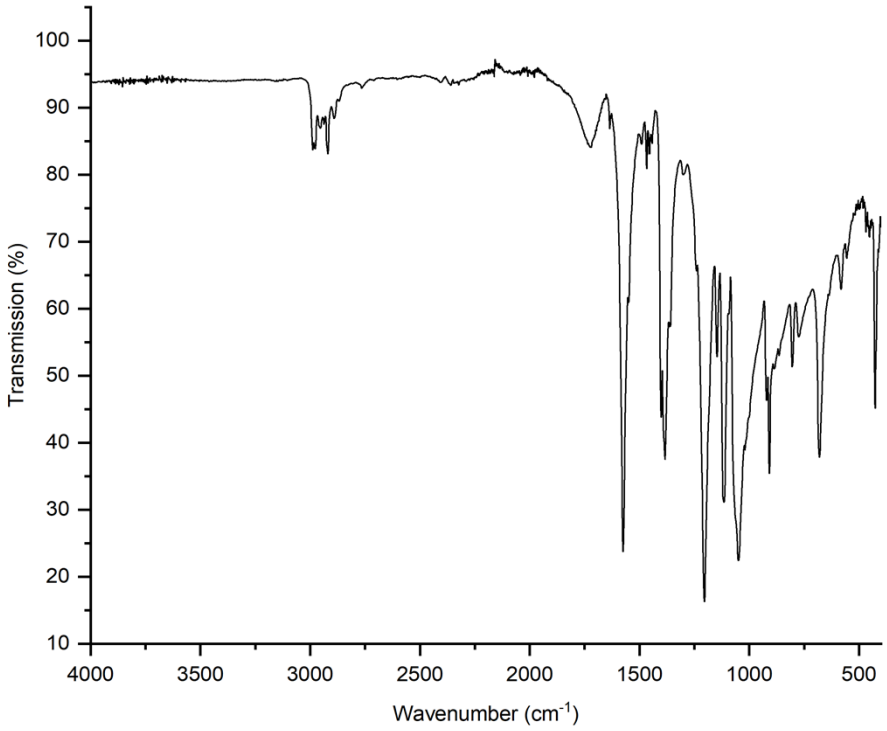

Figure S32: IR spectrum of **L_1K** (benchtop synthesis).

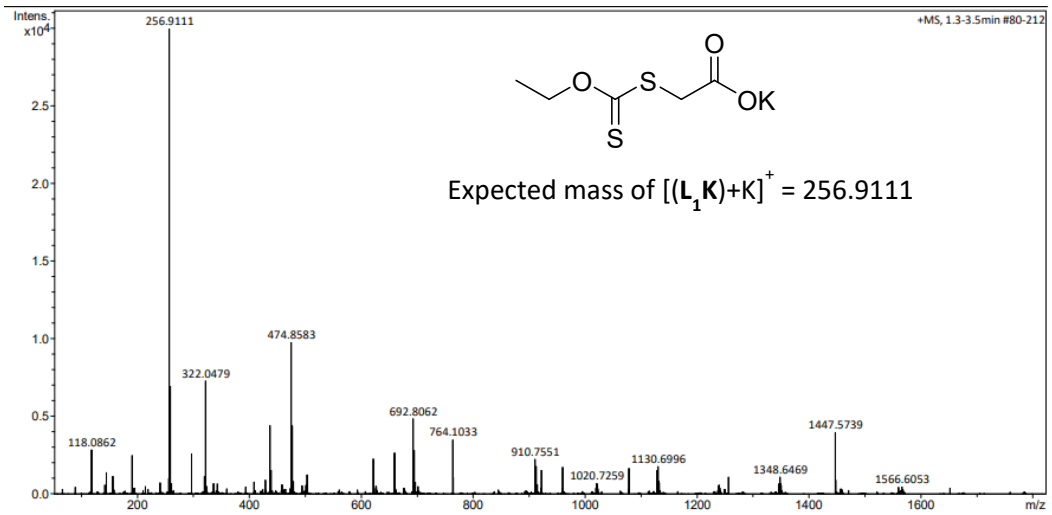

Figure S33: ESI-MS of **L_1K** (benchtop synthesis).

Characterisation data for L_2K

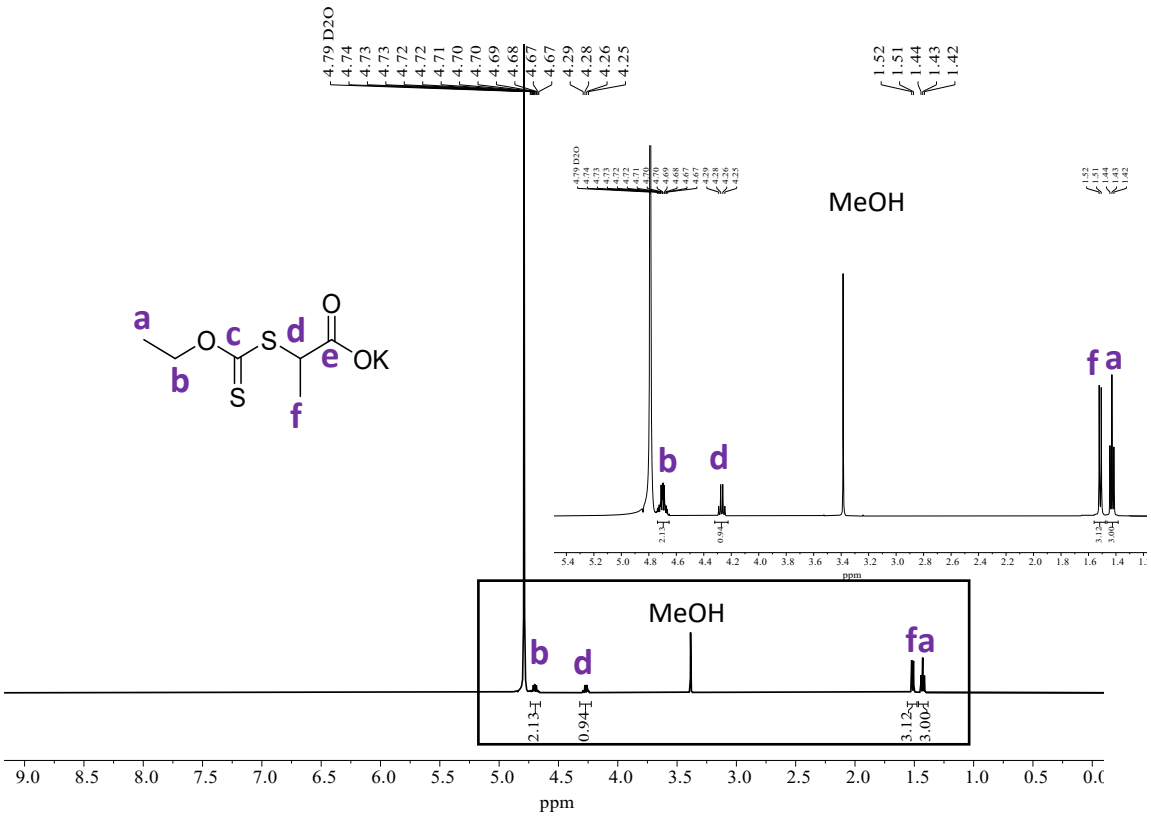

Figure S34: ^{1}H NMR spectrum of **L_2K** (air-sensitive synthesis) in D_2O (300 K).

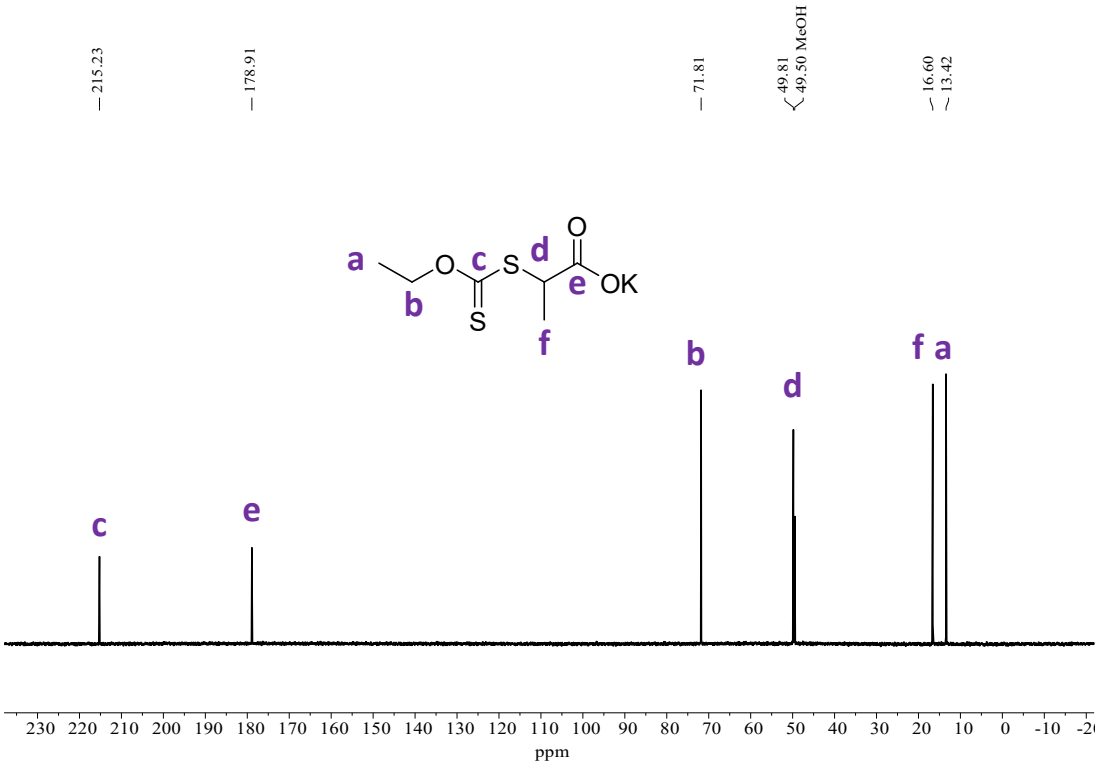

Figure S35: ^{13}C NMR spectrum of **L_2K** (air-sensitive synthesis) in D_2O (300 K).

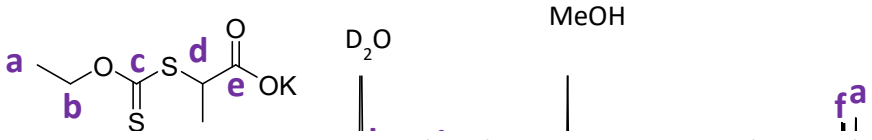

Figure S36: COSY NMR spectrum of **L_2K** (air-sensitive synthesis) in D_2O (300 K).

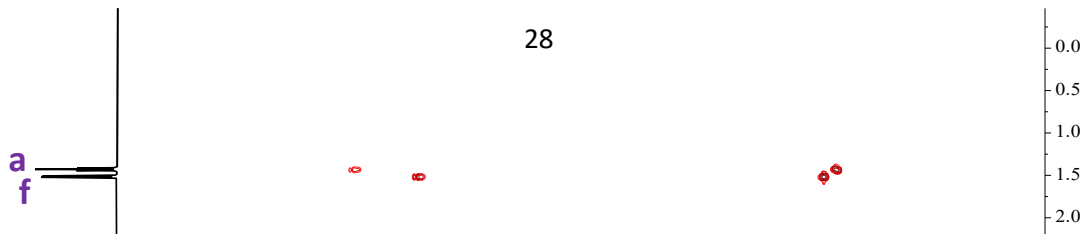

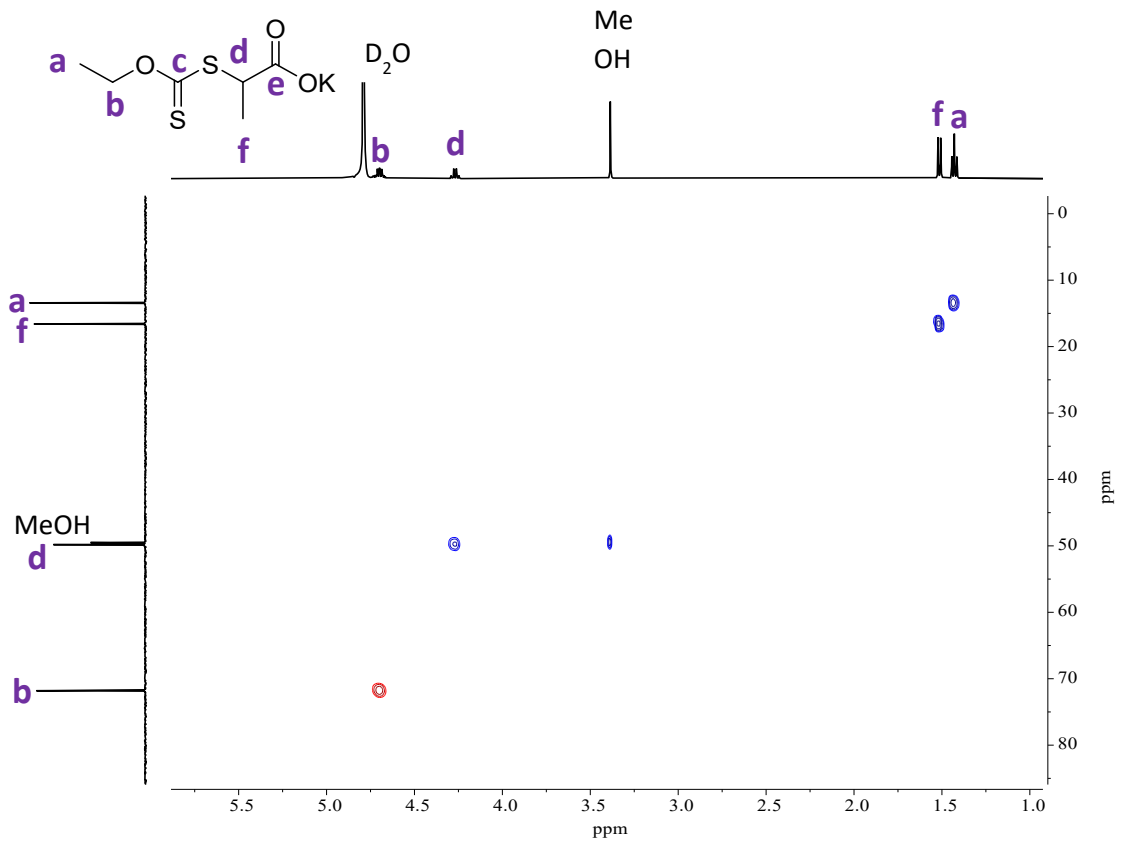

Figure S37: HSQC NMR spectrum of **L_2K** (air-sensitive synthesis) in D_2O (300 K).

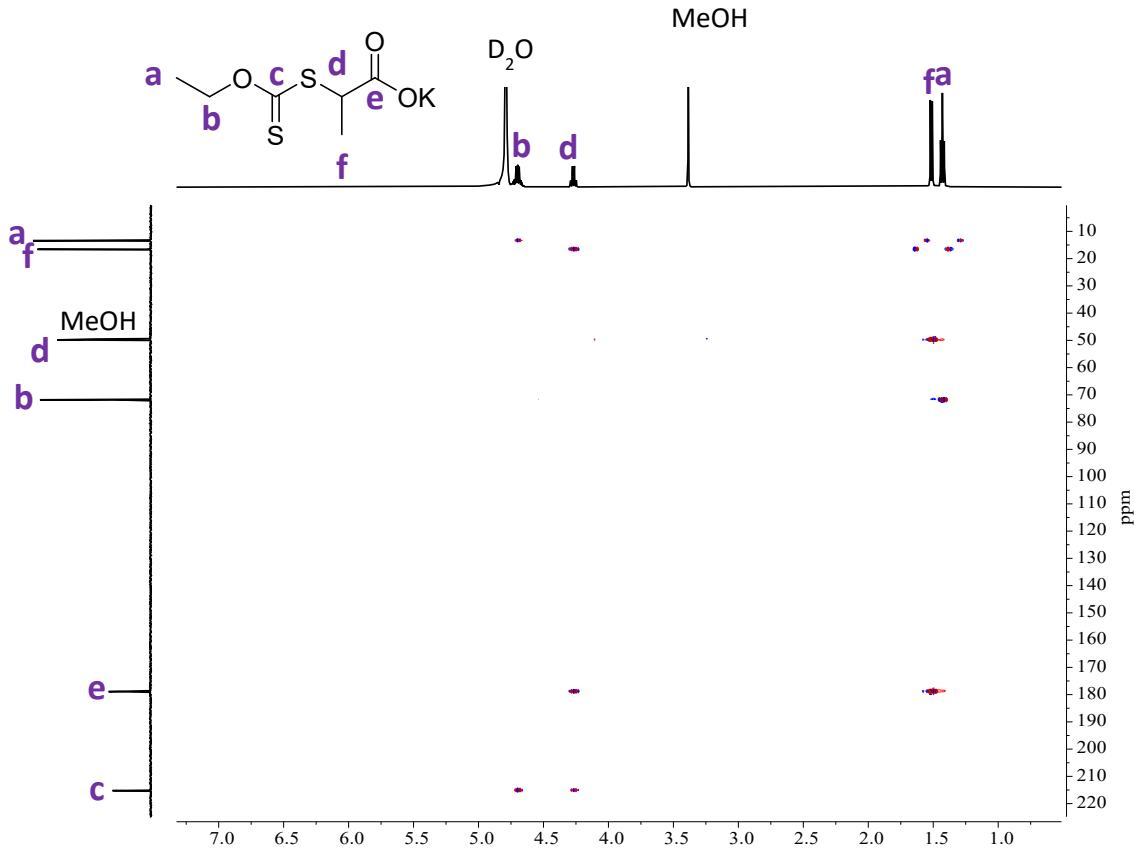

Figure S38: HMBC NMR spectrum of **L_2K** (air-sensitive synthesis) in D_2O (300 K).

Polymerisation characterisation data – polyesters prepared via epoxide/anhydride ROCOP

Representative NMR spectra for epoxide/anhydride ROCOP

Figure S39: Representative example ^{1}H NMR spectrum of crude poly(PA-*alt*-CHO) prepared with **L_1K** under air-sensitive conditions in $CDCl_3$ (300 K) showing monomer and polymer peaks.

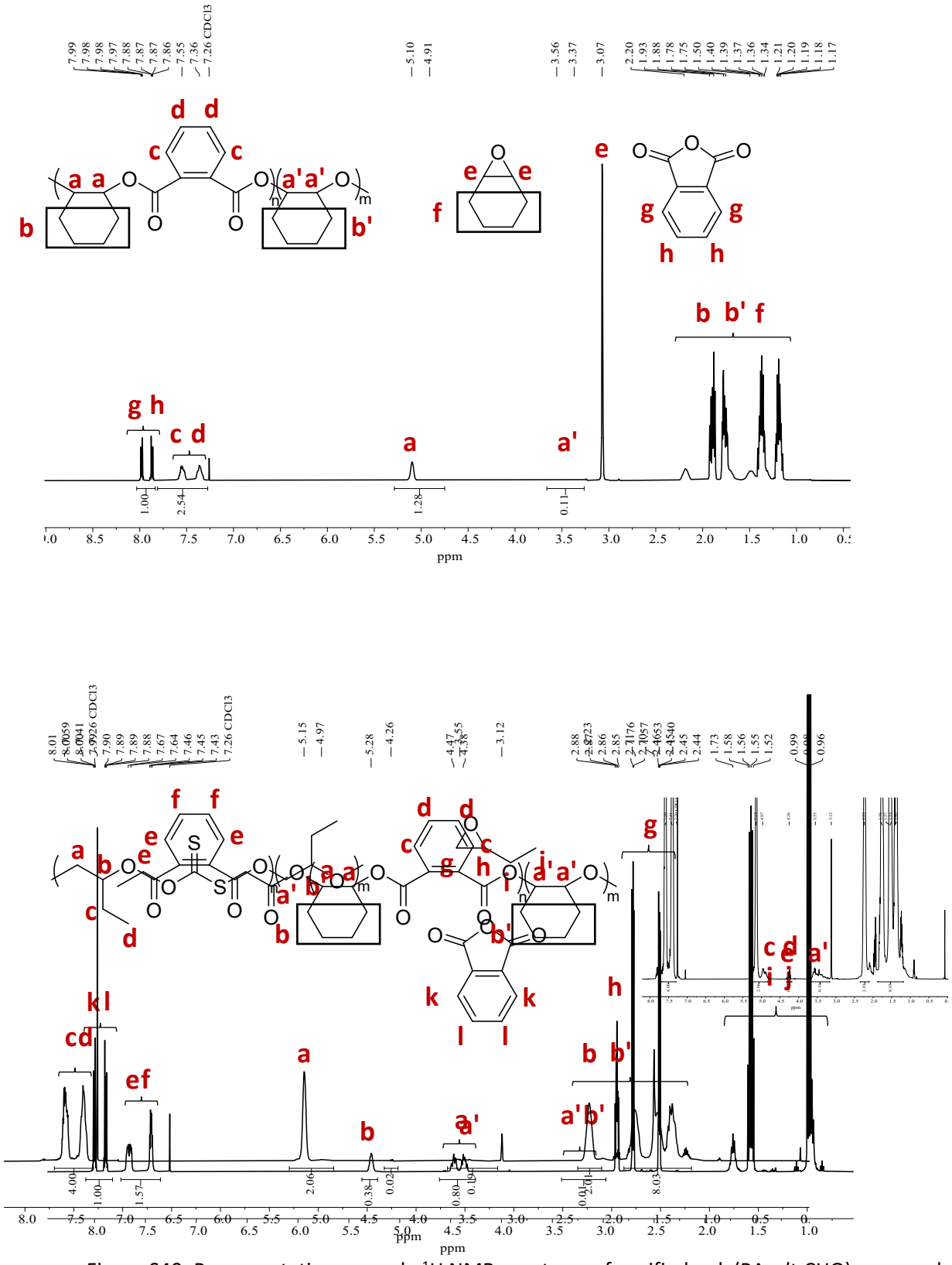

Figure S41: Representative example ^{1}H NMR spectrum of crude poly(PA-*alt*-EB) prepared with **L$_1$K** under air-sensitive conditions in $CDCl_3$ (300 K) showing monomer and polymer peaks.

Kinetic plots for epoxide/anhydride ROCOP

Figure S42: Zero order kinetic plot of ROCOP of PA and CHO by **L_1K** and **L_2K**.

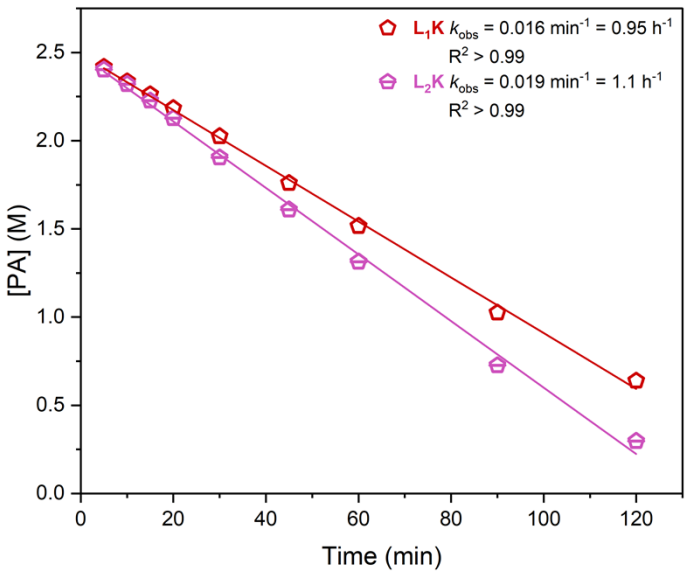

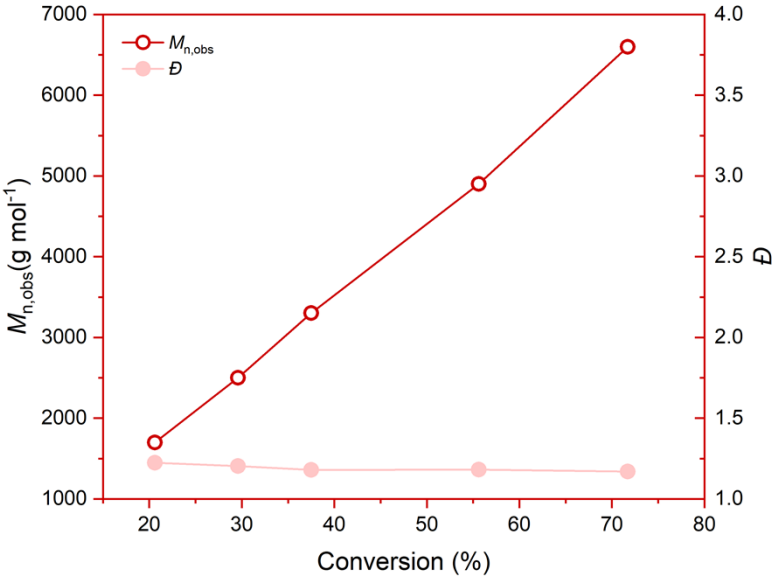

Figure S43**:** M_n and *Đ* versus PA conversion in PA/CHO ROCOP by **L_1K**.

Representative SEC traces for epoxide/anhydride ROCOP

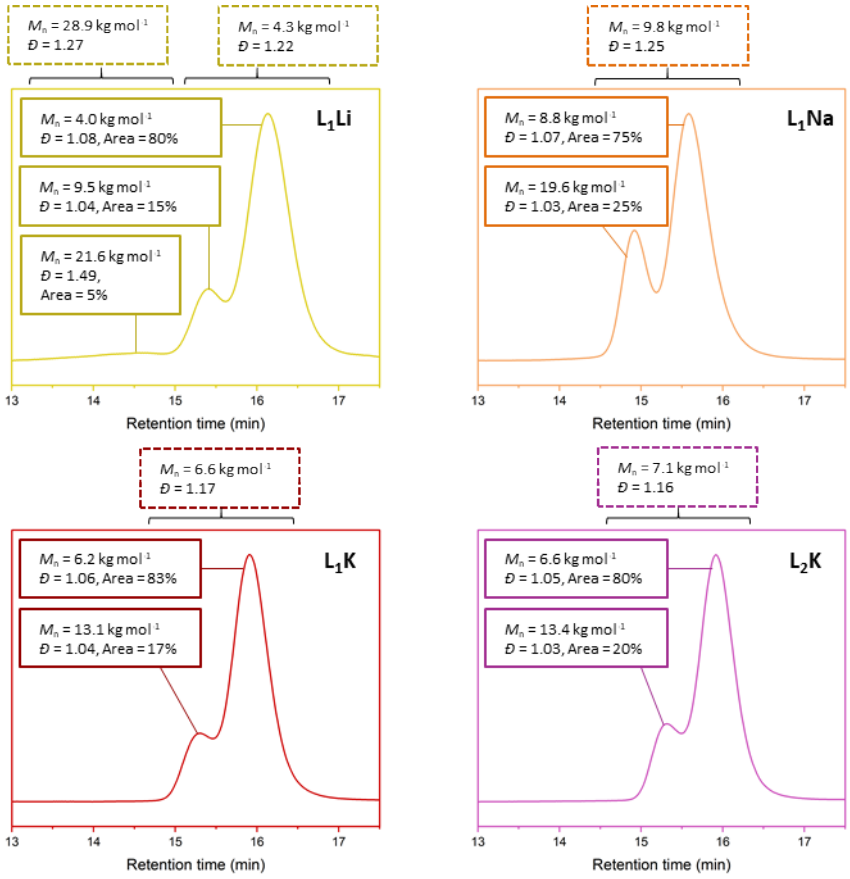

Figure S44: Deconvoluted SEC traces of ROCOP of PA and CHO by **LM** salts prepared under air-sensitive conditions. Peak deconvolution was performed using the template by the Konkolewicz group, provided by the Macromolecular Alliance for Community Resources and Outreach.

Representative MALDI-ToF analysis of poly(ester)-*block*-PVAc copolymers

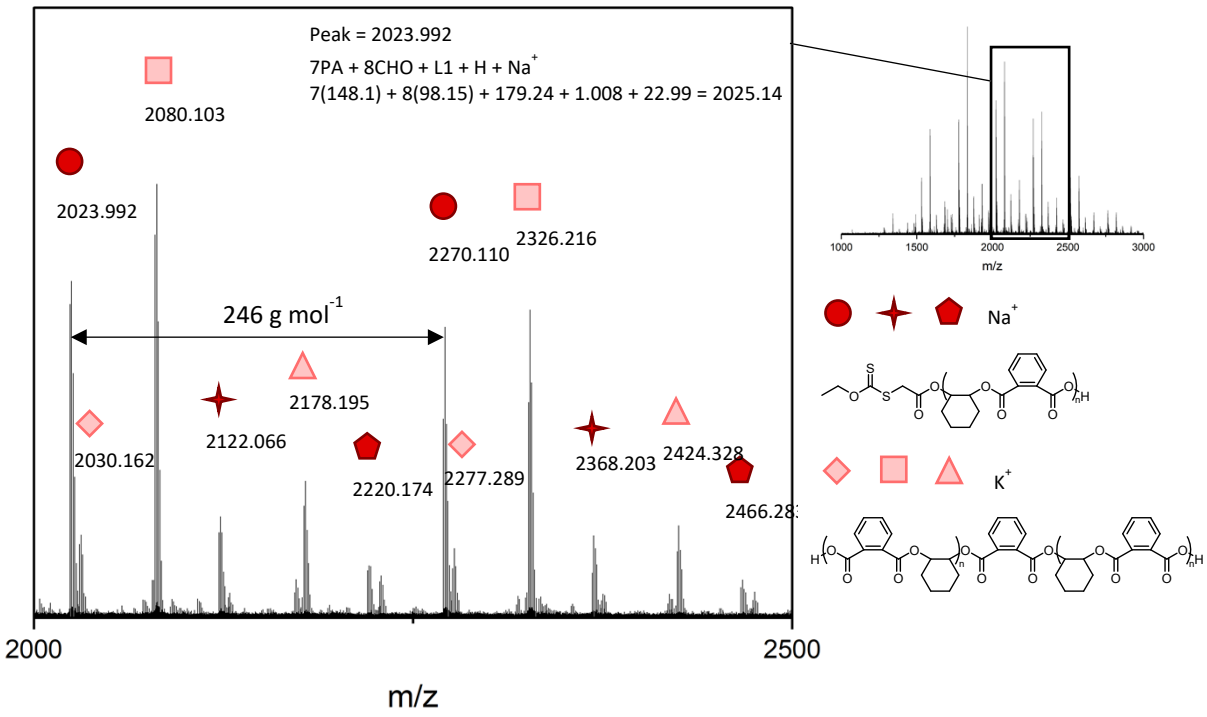

Figure S45: MALDI-ToF spectrum of poly(PA-*alt*-CHO) prepared with **L_1K** at 21% conversion, showing series with the expected RAFT end groups (red) and series initiated from diacid impurities (from ring-opened anhydride) (pink), as commonly observed for ROCOP across literature.[4–6]

Synthesis of poly(ester)-*block*-PVAc copolymers

Table S1: Conversion and SEC results of block copolymerisation of polyesters with vinyl acetate.

Entry	Macro-RAFT Polyester	Polyester M_n (kDa)	Temperature (°C)	Time (h)	[AIBN]:[Macro-RAFT]:VAc	Conv[a] (%)	$M_{n,obs}$[b] (kDa)	$Đ$[b]
1	**Poly(PA-*alt*-CHO)**[c]	14.6[f] 7.2	65	20	0.25:1:400	90	36.9[f] 14.2 7.2	1.78 1.04 1.07
2	**Poly(PA-*alt*-CHO)**[d]	1.8	65	19.5	0.20:1:100	63	49.5[f] 1.9	3.1 1.2
3	**Poly(PA-*alt*-EB)**[e]	1.8	65	19.5	0.20:1:100	45	43.2[f] 1.9	2.2 1.1

[a]Conversion calculated by ^{1}H NMR. [b]$M_{n,obs}$ and $Đ$ determined by SEC analysis in THF solvent, calibrated with narrow dispersity polystyrene standards. [c]Air-sensitive prepared polyester (Table 1, Entry 6 but with a reaction time of 2.5 h giving 83% conversion). [d]Benchtop prepared polyester (Table 2, Entry 4). [e]Benchtop prepared polyester (Table 2, Entry 2). [f]Bi- or multimodal traces observed; deconvoluted results reported. Peak deconvolution was performed using the template by the Konkolewicz group provided by the Macromolecular Alliance for Community Resources and Outreach.

Polymerisation characterisation data – synthesis of copolymers via ROCOP and RAFT

Representative NMR spectra

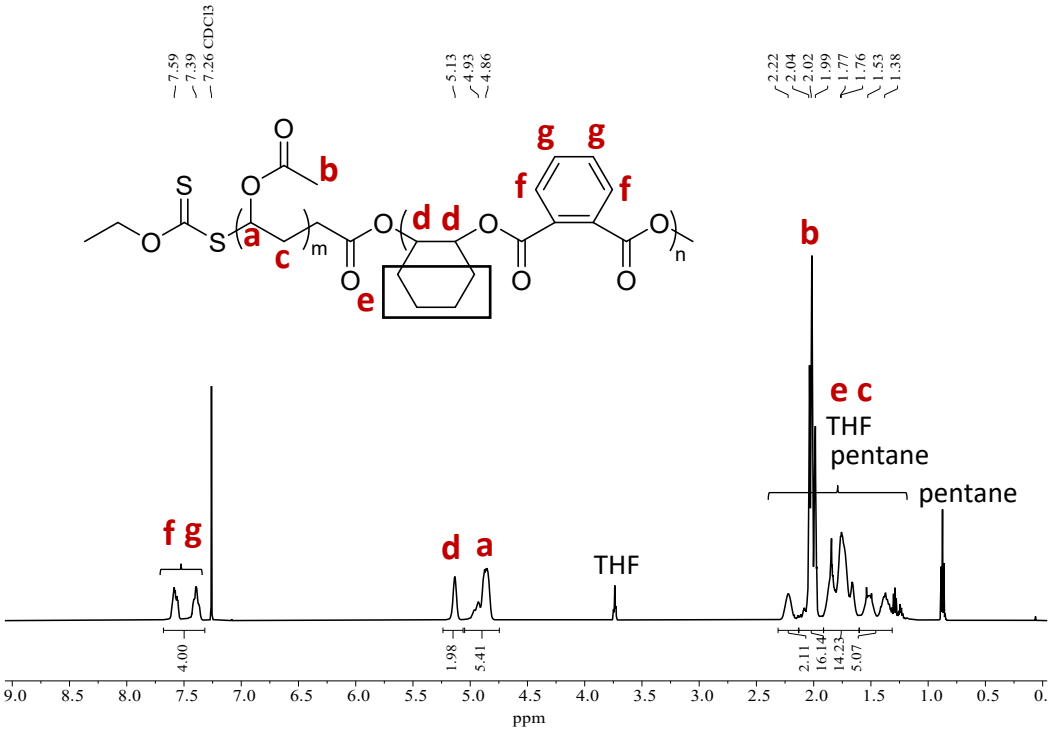

Figure S46: ^{1}H NMR spectrum of crude poly(PA-*alt*-CHO)-*block*-PVAc in $CDCl_3$ (300 K) (Table S1, Entry 1). The crude product contains a mixture of poly(PA-*alt*-CHO) and poly(PA-*alt*-CHO-*block*-PVAc (refer to manuscript for details).

Note on the potential for transesterification

The potential for transesterification between the polyester backbone and the vinyl acetate side-arms was considered, yet deemed unlikely. Firstly, the polymer samples remained soluble, and introducing cross-links via transesterification would significantly lower the solubility and increase the M_n. Secondly, no new carbonyl peaks were observed in the ^{13}C NMR spectrum for the poly(ester-*co*-acrylate) vs the corresponding polyester and polyacrylate homopolymer (Figure S43). Thirdly, poly(ester-*co*-acrylate) BCPs prepared *via* ROCOP-RAFT have been reported in literature, with no mention of transesterification.[7,8]

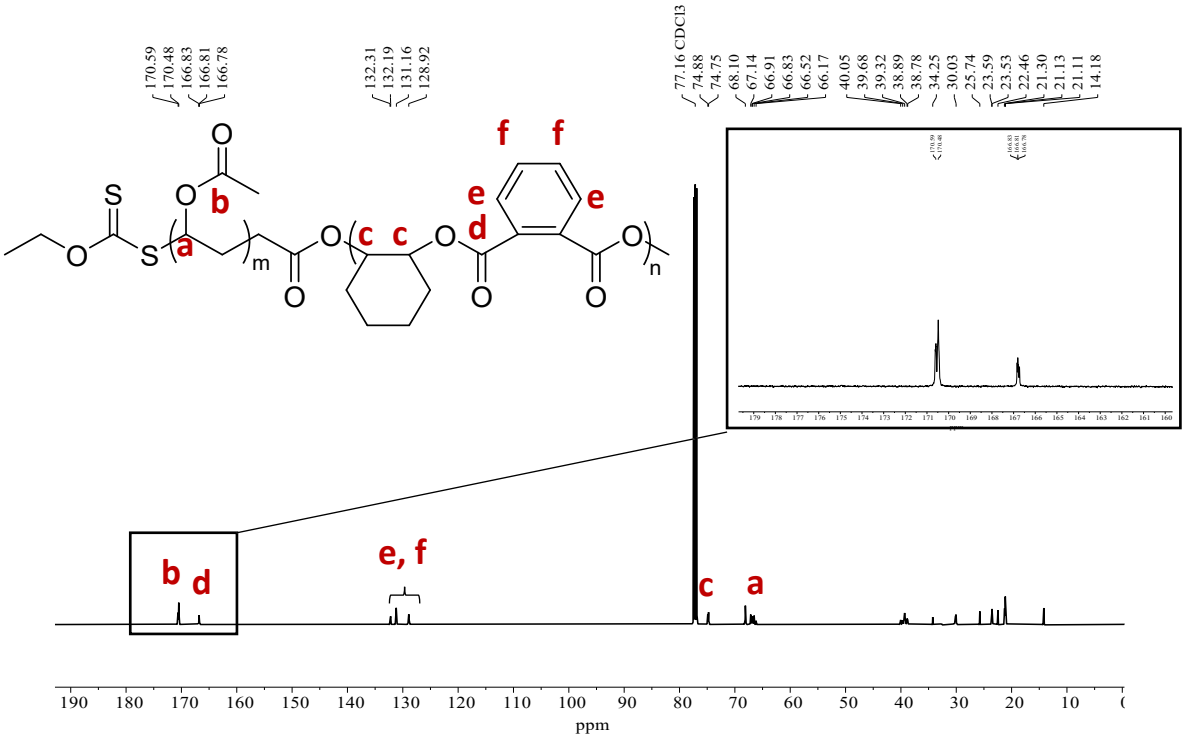

Figure S47: ^{13}C NMR spectrum of crude poly(PA-*alt*-CHO)-*block*-PVAc in $CDCl_3$ (300 K) (Table S1, Entry 1). The crude product mixture contains a mixture of poly(PA-*alt*-CHO) and poly(PA-*alt*-CHO-*block*-PVAc (refer to manuscript for details).

Figure S48: ^{1}H NMR spectrum of poly(PA-*alt*-EB)-*block*-PVAc in $CDCl_3$ (300 K) prepared using poly(PA-*alt*-EB) synthesised under benchtop conditions (Table S1, Entry 3). The crude product mixture contains a mixture of poly(PA-*alt*-EB) and poly(PA-*alt*-EB-*block*-PVAc (refer to manuscript for details).

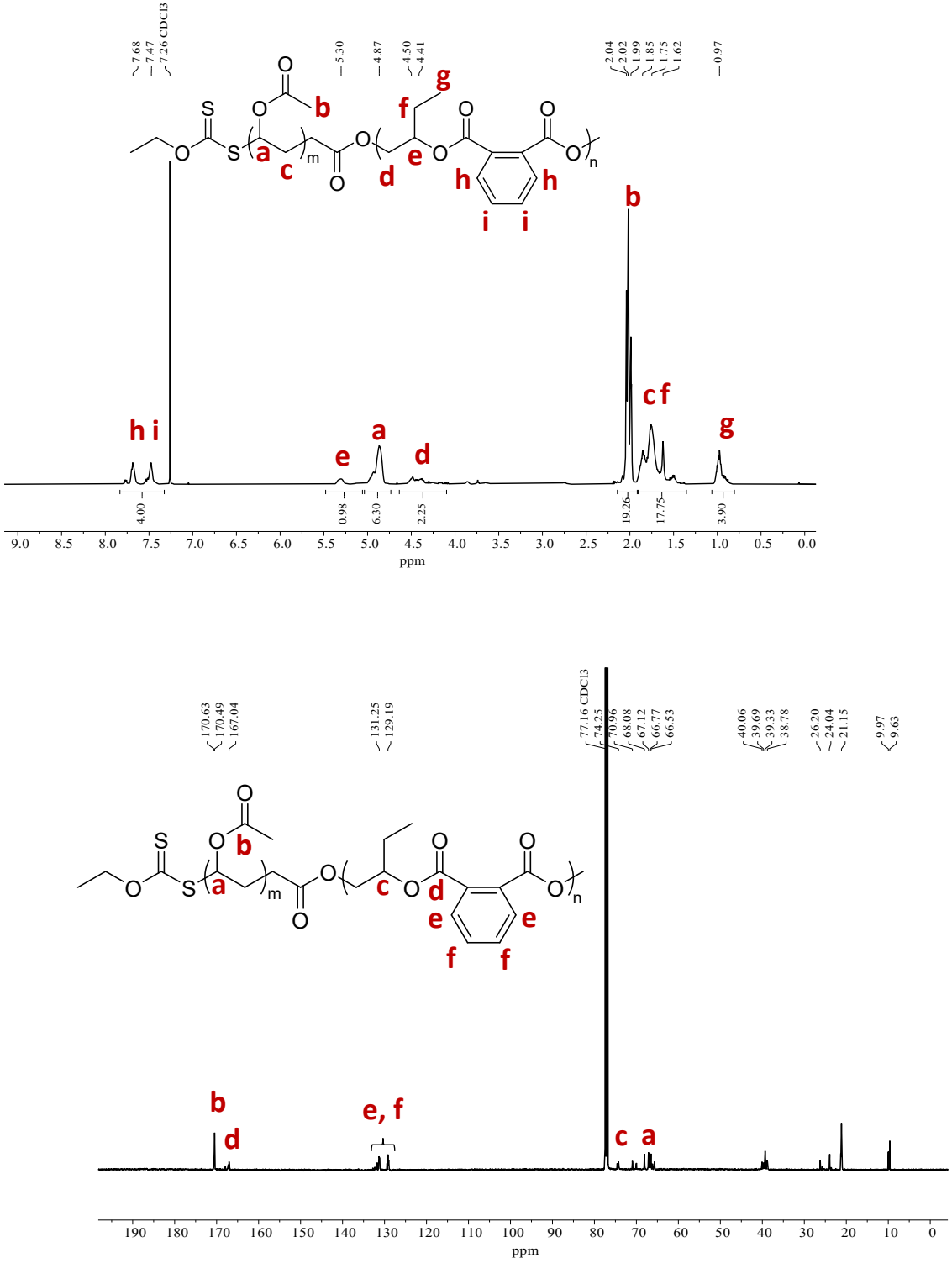

Figure S49: ^{13}C NMR spectrum of poly(PA-*alt*-EB)-*block*-PVAc in $CDCl_3$ (300 K) prepared using poly(PA-*alt*-EB) synthesised under benchtop conditions (Table S1, Entry 3). The crude product mixture contains a mixture of poly(PA-*alt*-EB) and poly(PA-*alt*-EB-*block*-PVAc (refer to manuscript for details).

DOSY NMR analysis: chain extension of polyester precursors *via* RAFT polymerisation

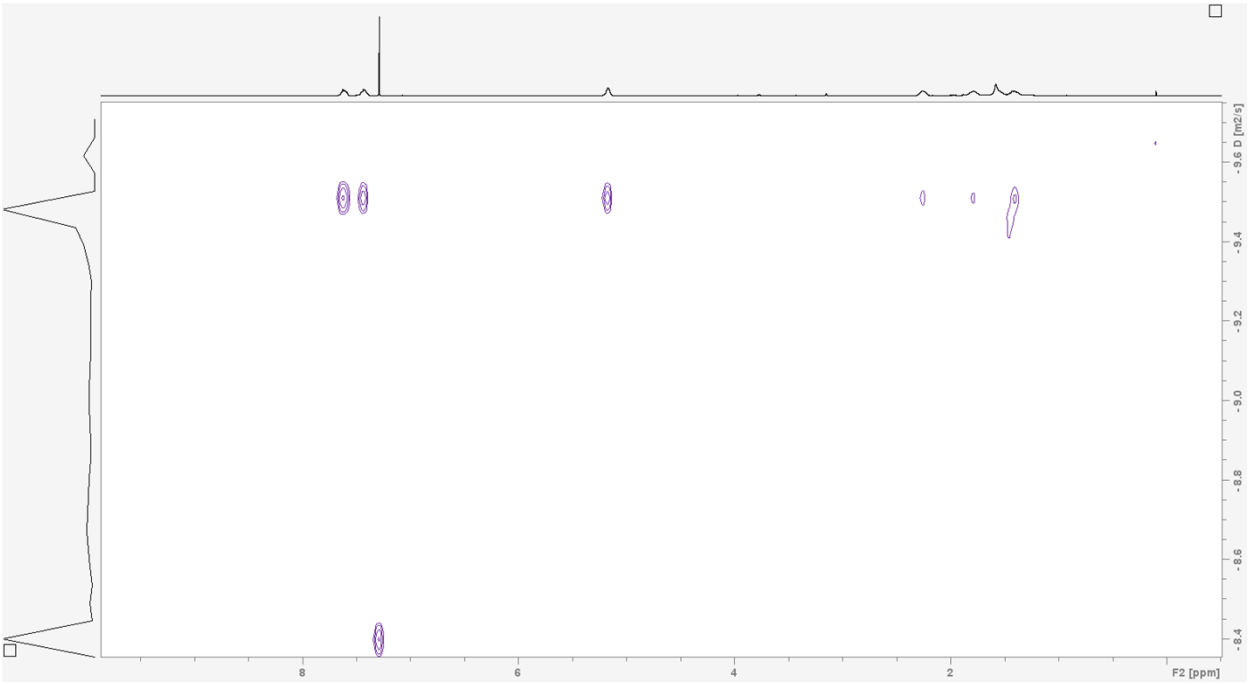

Figure S50: DOSY NMR spectrum of poly(PA-*alt*-CHO) precursor in $CDCl_3$ (300 K) (Table S1, Entry 1).

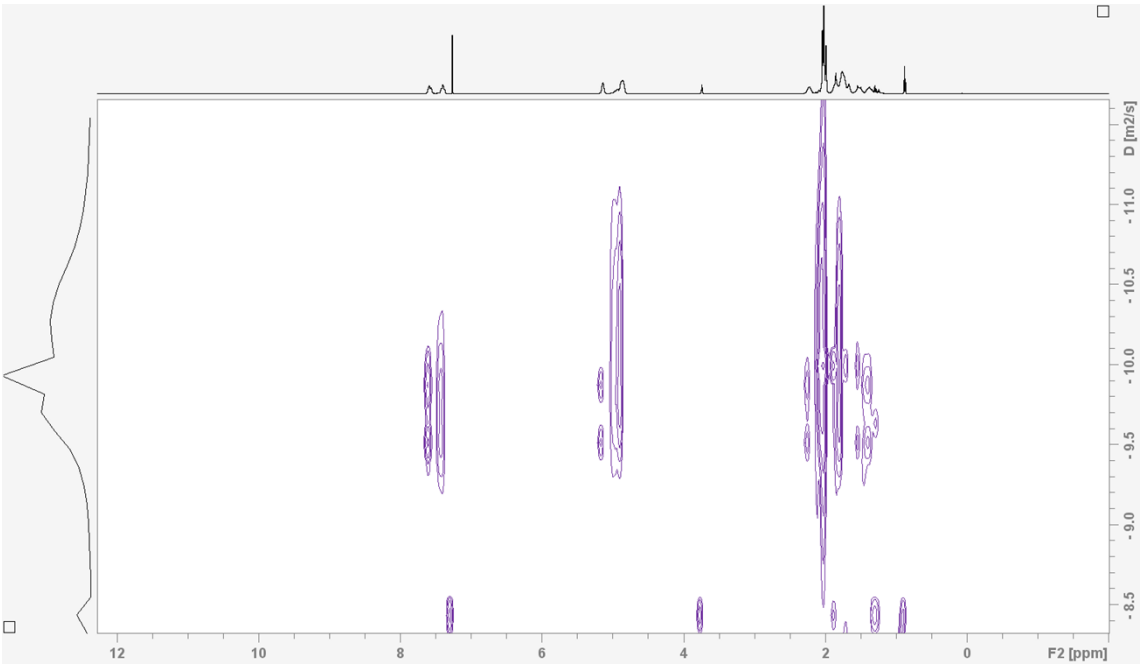

Figure S51: DOSY NMR spectrum of the crude product of block copolymerisation of poly(PA-*alt*-CHO) with VAc in $CDCl_3$ (300 K) (Table S1, Entry 1).

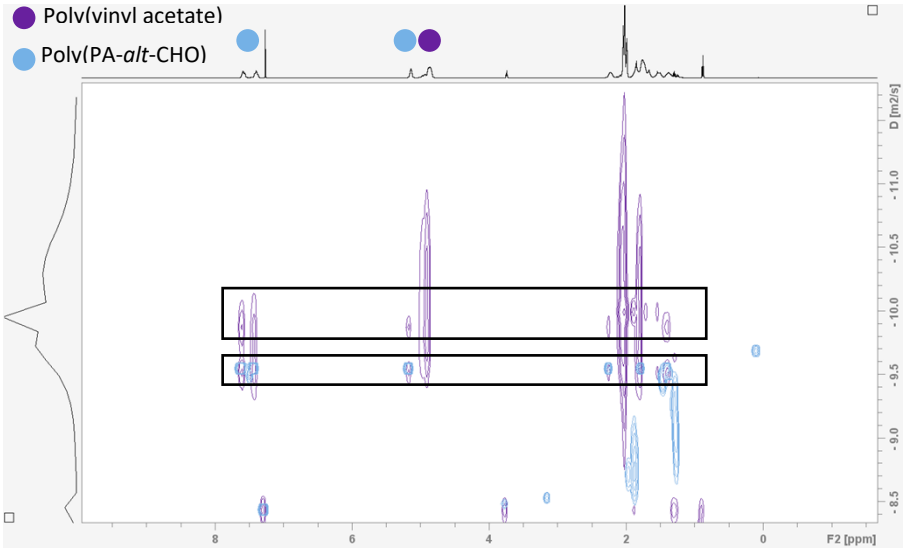

Figure S52: Overlaid DOSY spectra of poly(PA-*alt*-CHO) (Figure S50) (blue) prepared under air-sensitive conditions and the product of subsequent block copolymerisation with VAc (Figure S51) (purple), in $CDCl_3$ (300 K) (Table 2, Entry 3), showing two bands for the polyester. a) aligns with the polyester precursor i.e. is unreacted homopolymer and b) is a higher molecular weight species that aligns with the PVAc signal i.e. is a block copolymer.

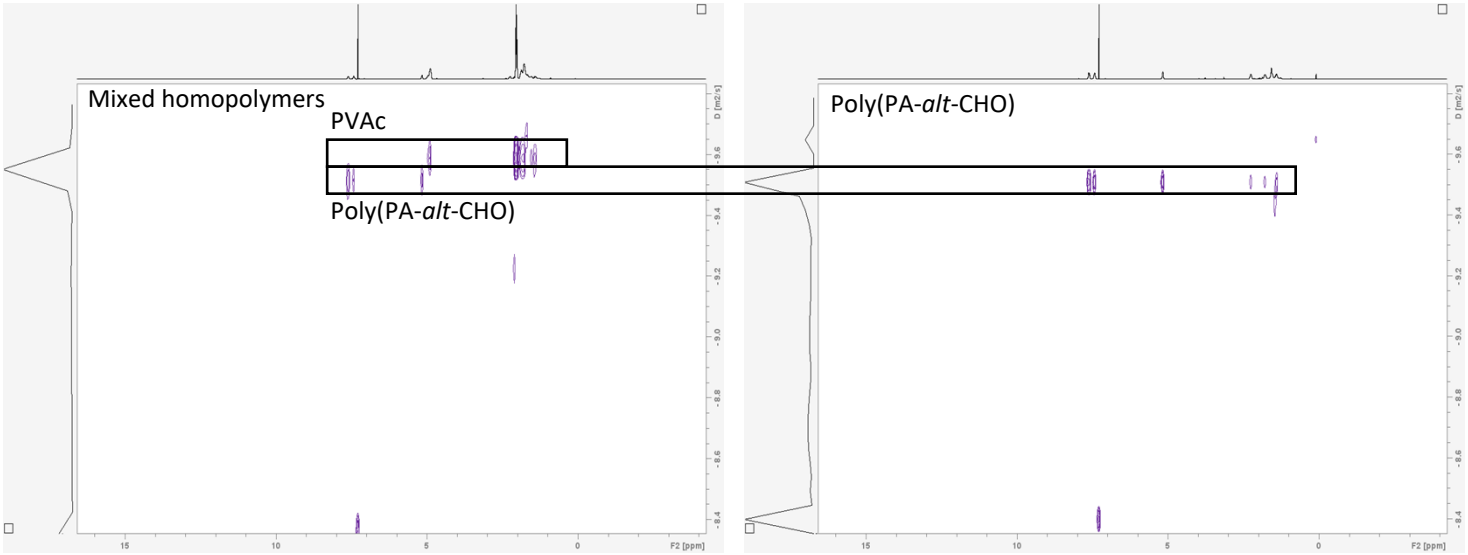

Figure S53: DOSY spectra of poly(PA-*alt*-CHO) (right) prepared under air-sensitive conditions (same sample as in Figure S52) and a mixture of the same poly(PA-*alt*-CHO) homopolymer ($M_{n,obs}$ = 6.6 kDa) with PVAc homopolymer ($M_{n,obs}$ = 10.7 kDa) (left), in $CDCl_3$ (300 K). The identical diffusion of the poly(PA-*alt*-CHO) in both samples contrasts with the increase observed upon copolymerisation with VAc (Figure S52).

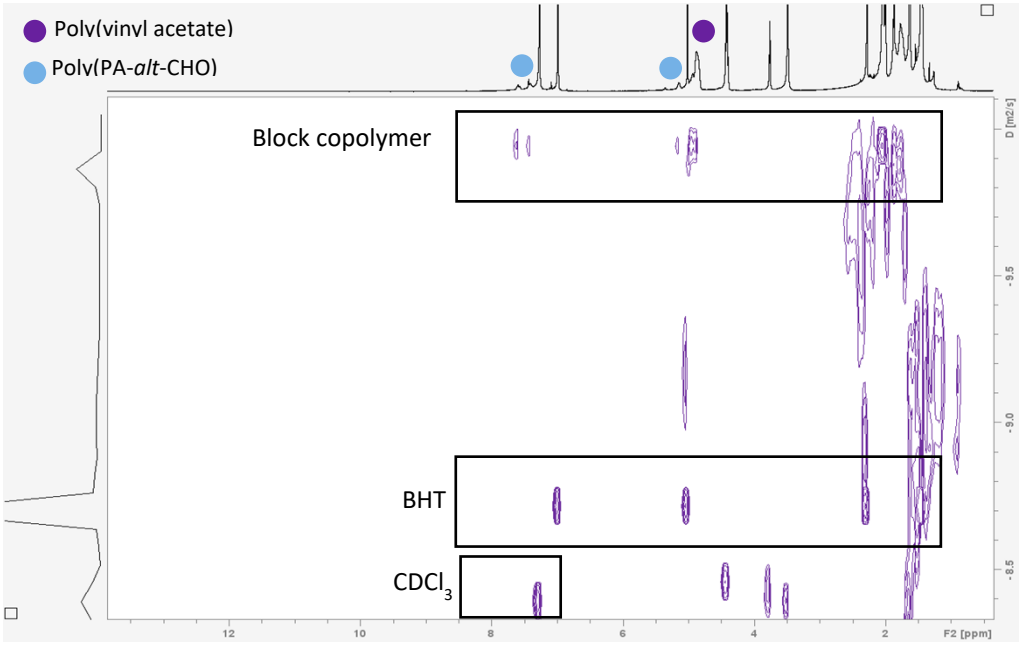

Figure S54: Expanded DOSY NMR spectrum of fractionated poly(PA-*alt*-CHO)-*block*-PVAc collected from SEC analysis (Figure 2, see purple SEC trace for fraction collected and purple DOSY plot), in $CDCl_3$ (300 K) (Table S1, Entry 1). BHT is present because it is used as a stabiliser in GPC grade THF; overlap with some polymer peaks (~ 1.5 ppm) leads to challenges with resolving different components in the mixture in this region of the spectrum.

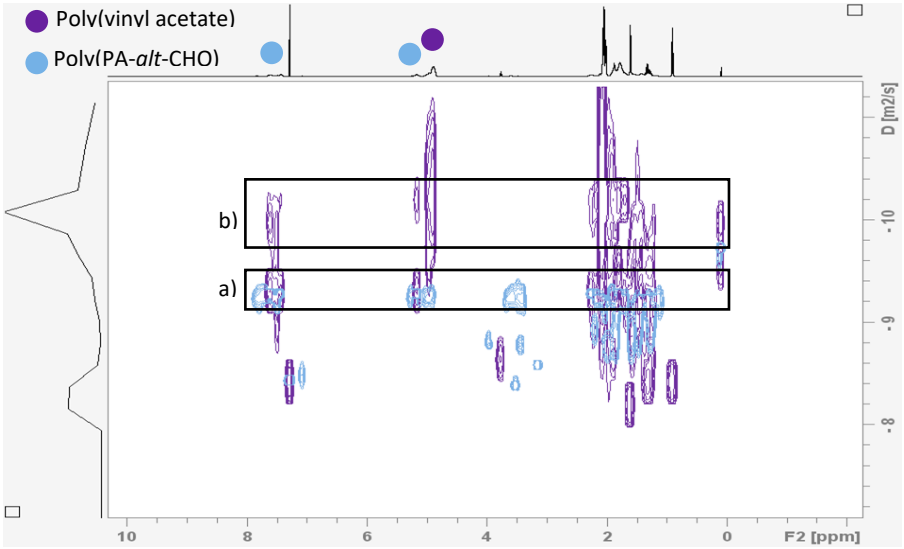

Figure S55: Overlaid DOSY spectra of benchtop prepared poly(PA-*alt*-CHO) (blue) and the product of subsequent block copolymerisation with VAc (purple), in $CDCl_3$ (300 K) (Table S1, Entry 2), showing two bands for the polyester. a) aligns with the polyester precursor i.e. is unreacted homopolymer and b) is a higher molecular weight species that aligns with the PVAc signal i.e. is a block copolymer.

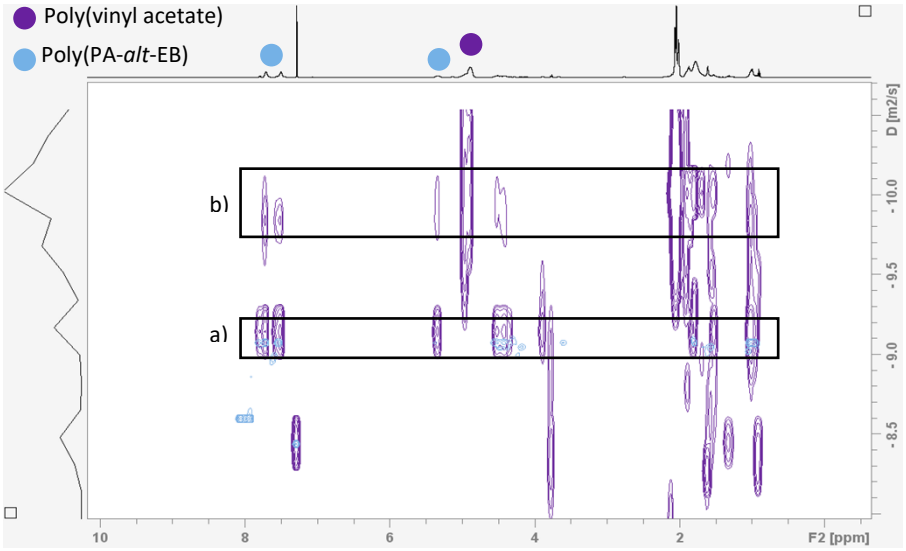

Figure S56: Overlaid DOSY spectra of benchtop prepared poly(PA-*alt*-EB) (blue) and the result of block copolymerisation with VAc (purple), in $CDCl_3$ (300 K) (Table S1, Entry 3), showing two bands for the polyester. a) aligns with the polyester precursor i.e. is unreacted homopolymer and b) is a higher molecular weight species that aligns with the PVAc signal i.e. is a block copolymer.

Representative SEC traces for the copolymerisation of polyesters with vinyl acetate

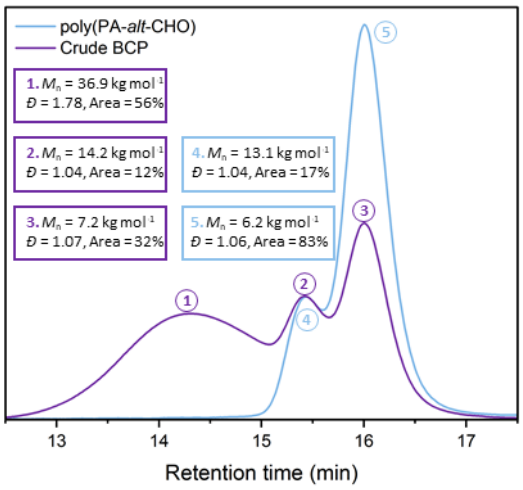

Figure S57**:** Overlaid SEC traces of the crude product from vinyl acetate RAFT polymerisation from poly(PA-*alt*-CHO) prepared under air-sensitive conditions (purple) (Table S1, Entry 1, main manuscript Fig. 2a) and the poly(PA-*alt*-CHO) precursor (blue). Both traces have been normalised to the high M_n shoulder peak of poly(PA-*alt*-CHO) (peaks 2 and 4); this shoulder is attributed to telechelic hydroxyl capped polyester that would remain unreacted in the RAFT polymerisation of VAc. In contrast, peak 5 is the main polyester peak containing the macro-RAFT functionality. The relative decrease of intensity from peak 5 to peak 3 after block copolymerisation provides further support for the reaction of RAFT functional groups to form BCPs. Deconvoluted molecular weights from the block copolymerisation are shown. Peak deconvolution was performed using the template by the Konkolewicz group provided by the Macromolecular Alliance for Community Resources and Outreach.

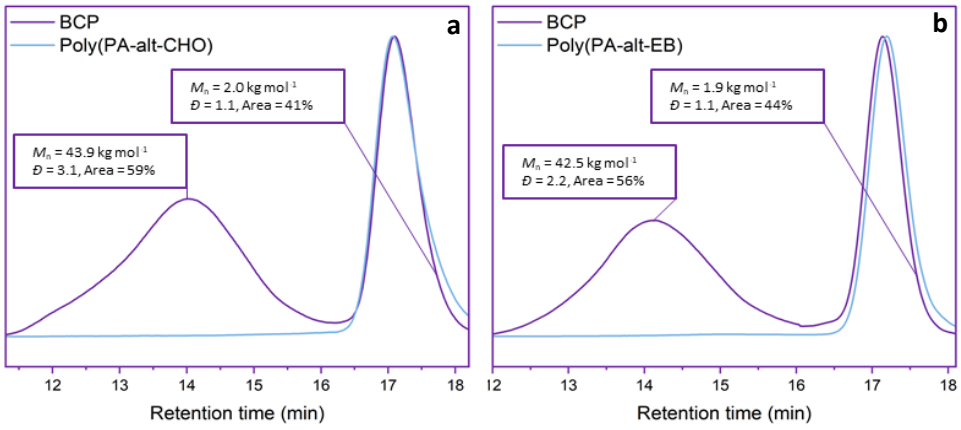

Figure S58: SEC traces of the crude product from vinyl acetate RAFT polymerisation from a) poly(PA-*alt*-CHO) (Table S1, Entry 2) and b) poly(PA-*alt*-EB) (Table S1, Entry 3) prepared under benchtop conditions (purple), overlaid with the respective polyester precursor (blue). Deconvoluted molecular weights from the block copolymerisation are shown. Peak deconvolution was performed using the template by The Konkolewicz group provided by the Macromolecular Alliance for Community Resources and Outreach.

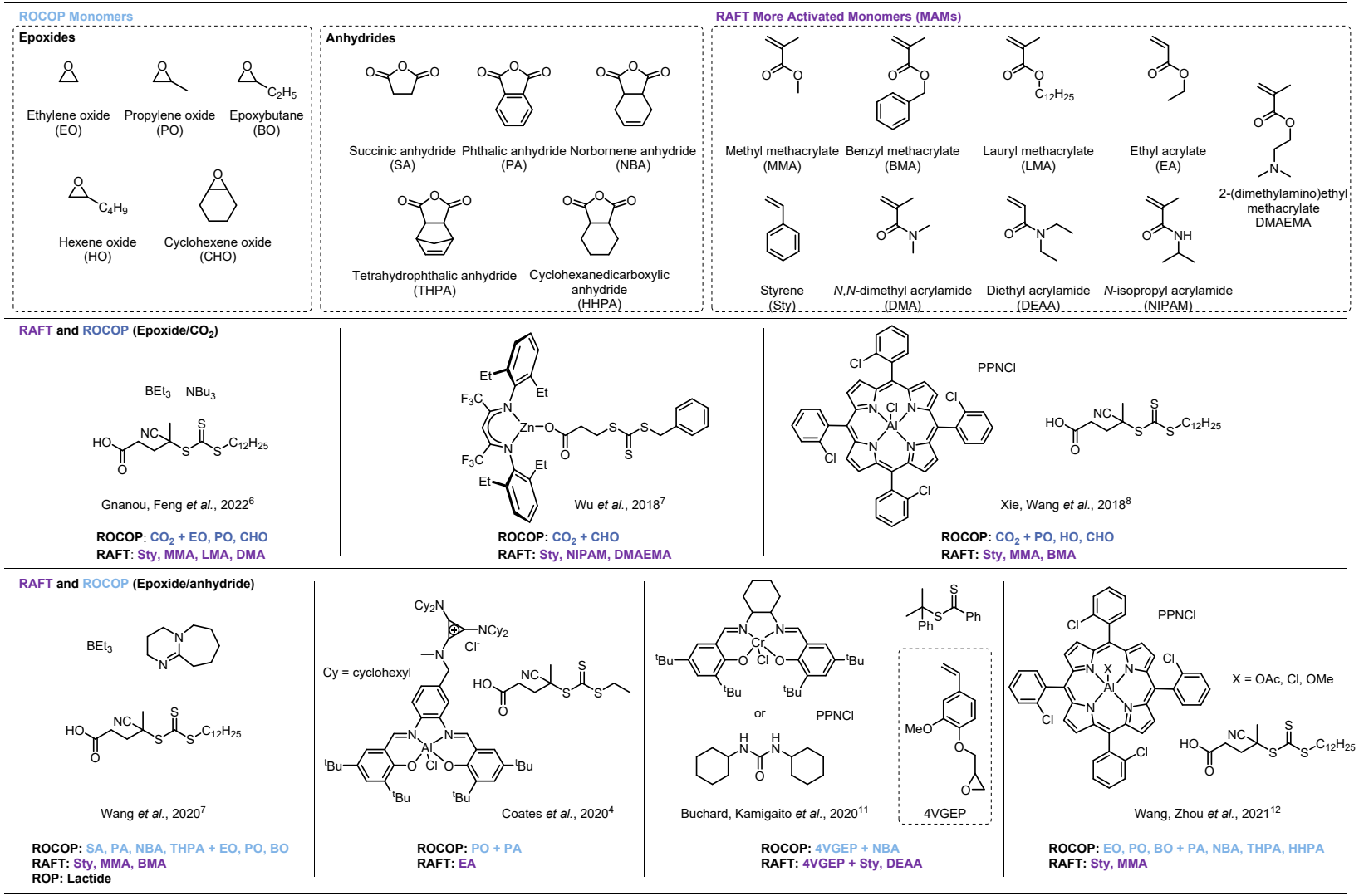

Figure S59: Overview of bifunctional systems reported in literature, and the corresponding monomer combinations used to synthesise ROCOP-RAFT BCPs (all carried out under air-sensitive conditions). (Note these reference numbers refer to the ESI; the same references are given as reference numbers 10-16 in the main manuscript).[4,7,9–13]

References

1 G. R. Fulmer, A. J. M. Miller, N. H. Sherden, H. E. Gottlieb, A. Nudelman, B. M. Stoltz, J. E. Bercaw and K. I. Goldberg, *Organometallics*, 2010, **29**, 2176–2179.

2 S. E. Edwards, S. Flynn, J. J. Hobson, P. Chambon, H. Cauldbeck and S. P. Rannard, *RSC Adv*, 2020, **10**, 30463–30475.

3 Q. Huang and S. Z. Zard, *Org. Lett.*, 2018, **20**, 1413–1416.

4 C. A. L. Lidston, B. A. Abel and G. W. Coates, *J. Am. Chem. Soc.*, 2020, **142**, 20161–20169.

5 W. T. Diment, G. L. Gregory, R. W. F. Kerr, A. Phanopoulos, A. Buchard and C. K. Williams, *ACS Catal.*, 2021, **11**, 12532–12542.

6 R. Xie, Y. Y. Zhang, G. W. Yang, X. F. Zhu, B. Li and G. P. Wu, *Angew. Chem. - Int. Ed.*, 2021, **311121**, 19253–19261.

7 S. Zhu, Y. Zhao, M. Ni, J. Xu, X. Zhou, Y. Liao, Y. Wang and X. Xie, *ACS Macro Lett.*, 2020, **9**, 204–209.

8 Y. Wang, Y. Zhao, S. Zhu, X. Zhou, J. Xu, X. Xie and R. Poli, *Angew. Chem.*, 2020, **132**, 6044–6050.

9 N. Patil, Y. Gnanou and X. Feng, *Polym. Chem.*, 2022, **13**, 2988–2998.

10 Y.-Y. Zhang, G.-W. Yang and G.-P. Wu, *Macromolecules*, 2018, **51**, 3640–3646.

11 Y. Wang, Y. Zhao, Y. Ye, H. Peng, X. Zhou, X. Xie, X. Wang and F. Wang, *Angew. Chem. - Int. Ed.*, 2018, **57**, 3593–3597.

12 T. M. McGuire, M. Miyajima, M. Uchiyama, A. Buchard and M. Kamigaito, *Polym. Chem.*, 2020, **11**, 5844–5850.

13 Y. Zhao, S. Zhu, X. Li, X. Zhao, J. Xu, B. Xiong, Y. Wang, X. Zhou and X. Xie, *CCS Chem.*, 2021, **4**, 122–131.